

Non-coding RNAs and the biology underpinning potential new precision medicines in cholangiocarcinoma

Chiara Braconi, MD PhD

*Lord Kelvin Adam Smith Reader
Hepatobiliary Oncology Group Leader
University of Glasgow*

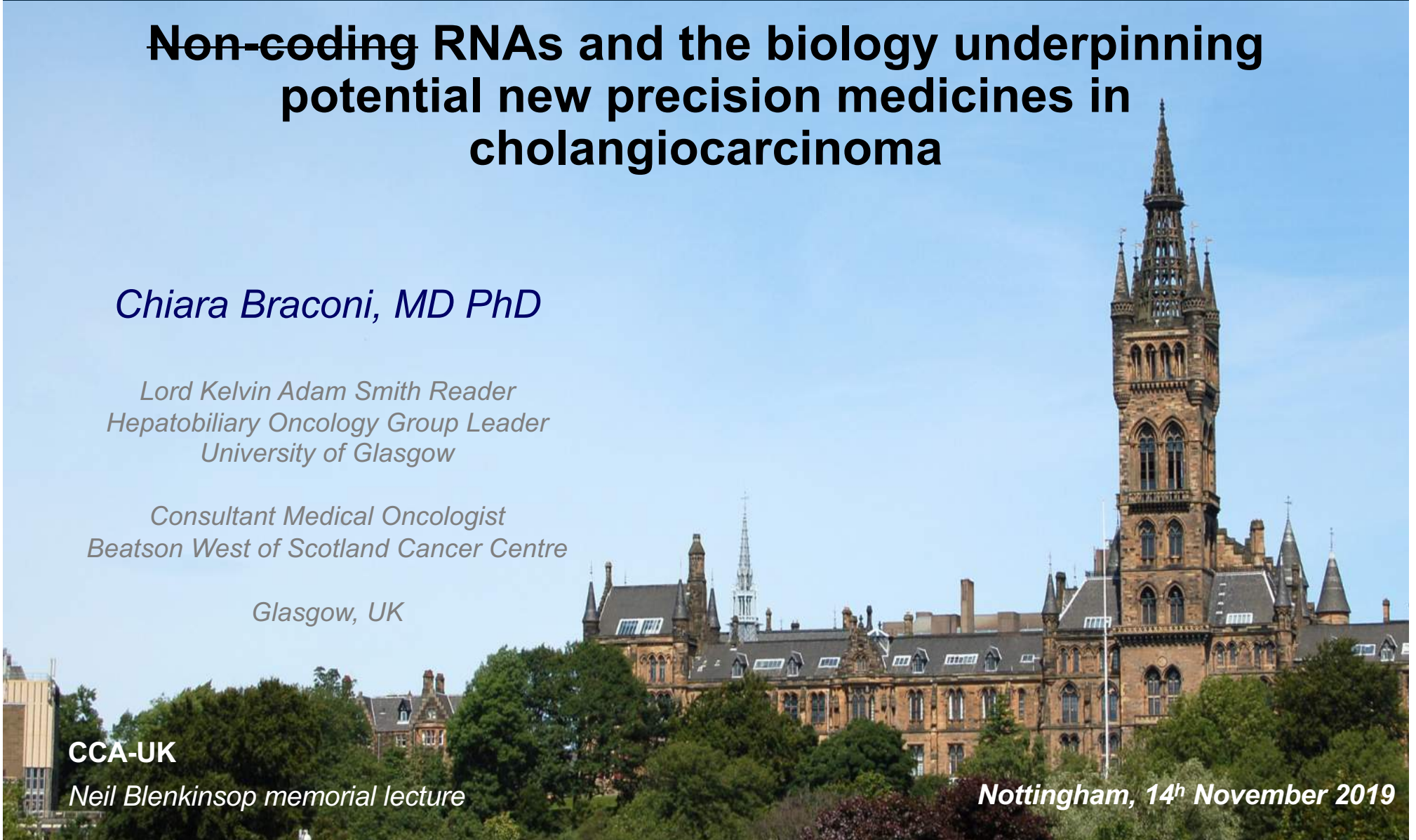
*Consultant Medical Oncologist
Beatson West of Scotland Cancer Centre*

Glasgow, UK

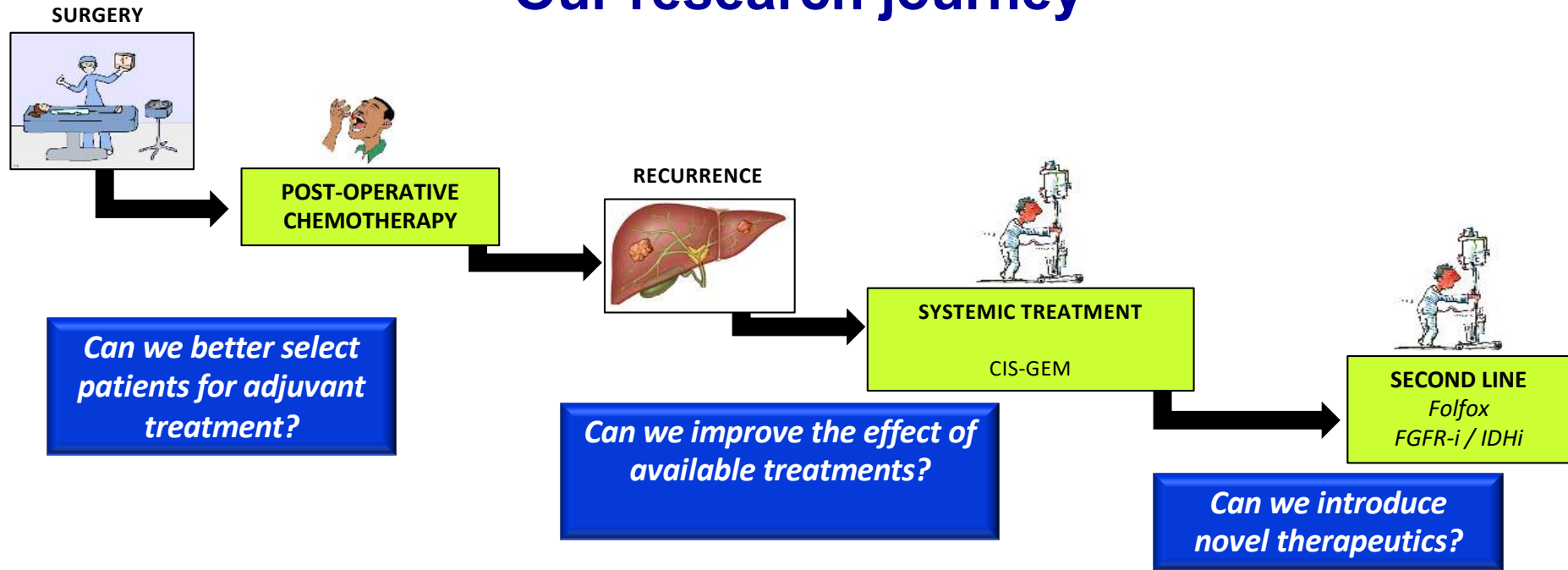
CCA-UK

Neil Blenkinsop memorial lecture

Nottingham, 14th November 2019



Our research journey



Immune-related transcripts as prognostic and predictive factors

MIR1249 as mediator of chemo-resistance

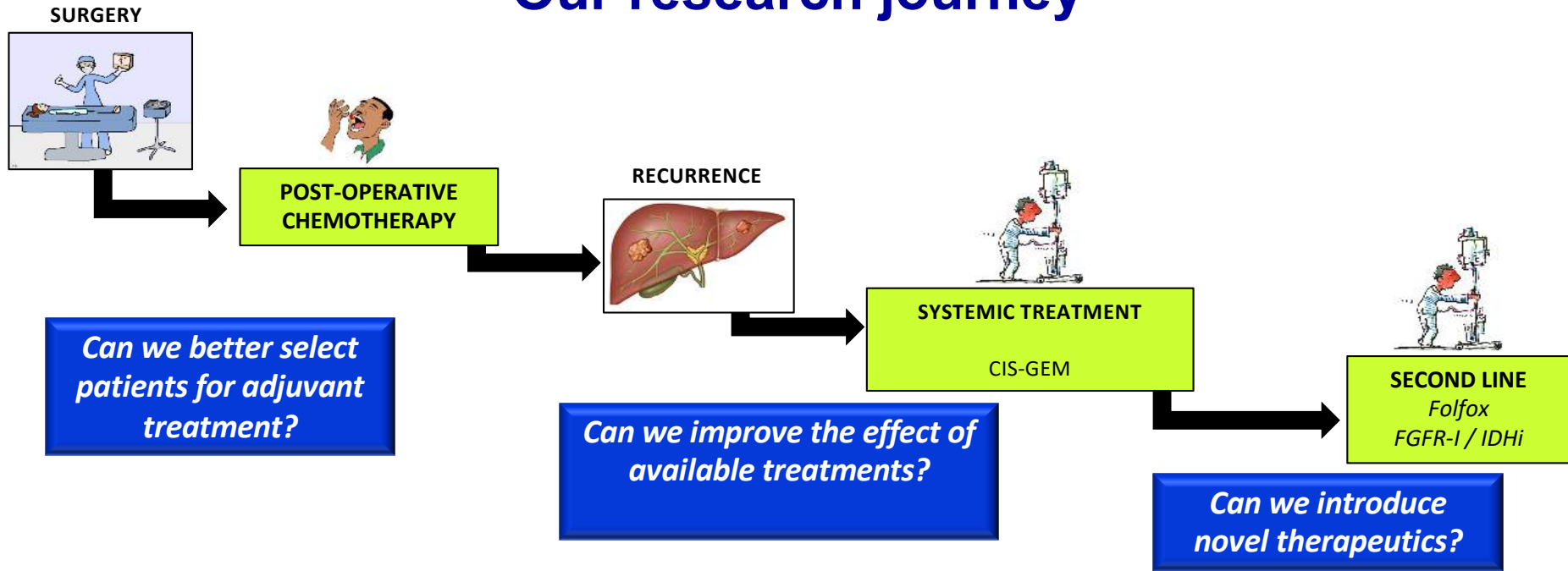
A.L.A.N. score

UC.158 as biomarker for Wnt-i

MIR21 as biomarker for HSP90-i

Patient derived organoids

Our research journey



Immune-related transcripts as prognostic and predictive factors

MIR1249 as mediator of chemo-resistance

A.L.A.N. score

UC.158 as biomarker for Wnt-i

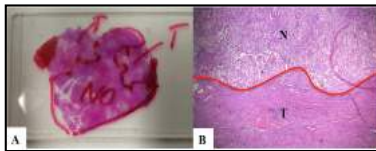
MIR21 as biomarker for HSP90-i

Patient derived organoids



Is the immune-related transcriptome altered in resected tumours?

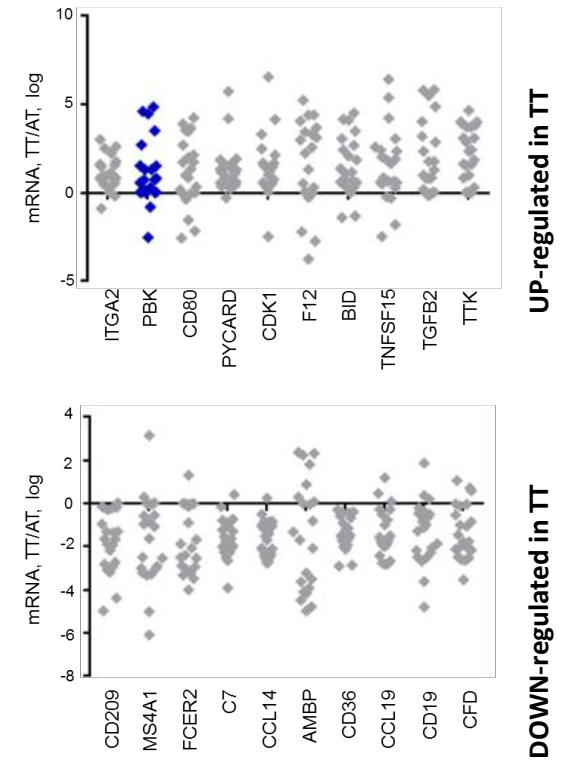
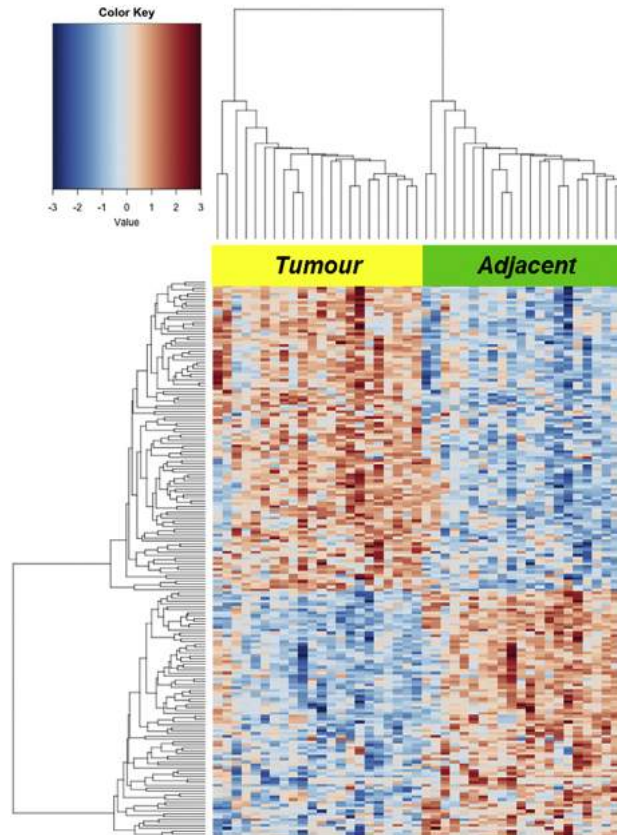
Exploratory set of FFPE resected tumours (N=22)



Microscopic dissection TT and AT

Immune profiling in TT and AT (770 immune-related genes)

Deregulation of the immune transcripts in resected BTC



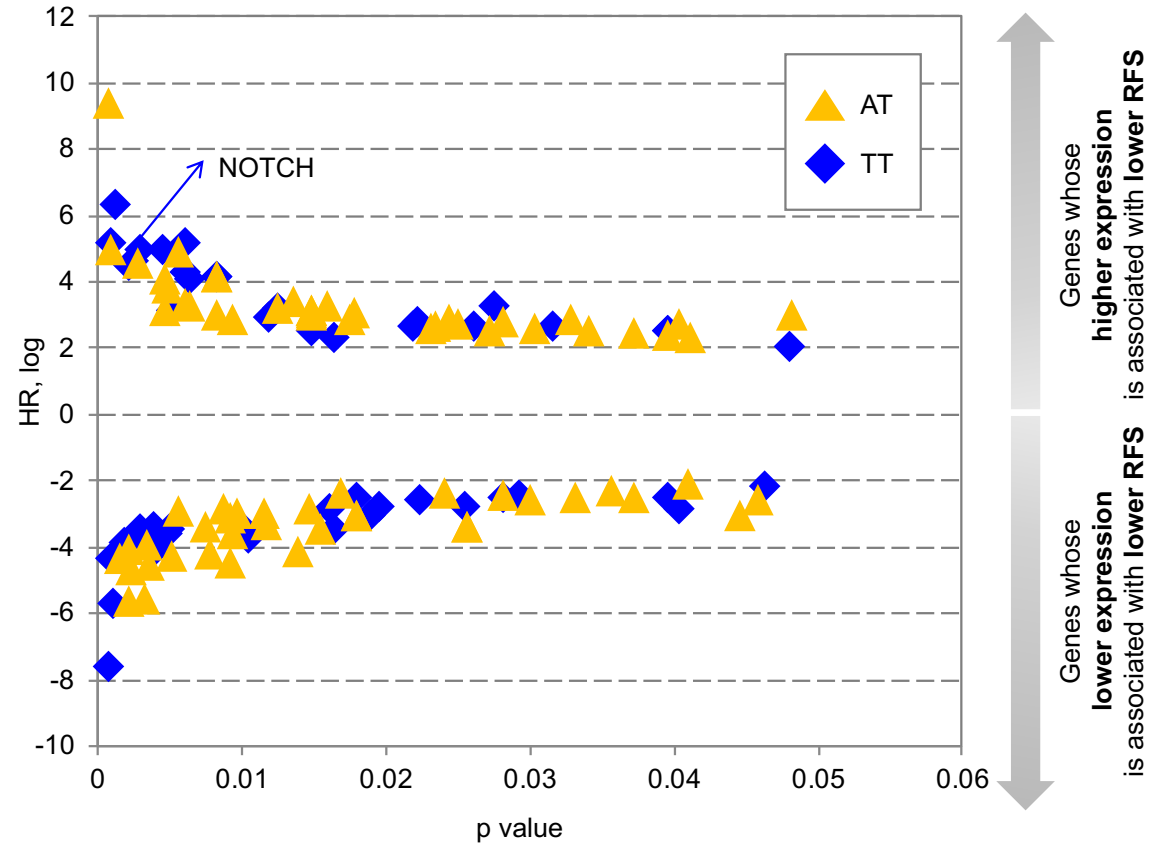
Risk of relapse is associated with a greater number of genes deregulated in the peritumoural area

Seed and soil theory



SEED = TUMOUR (TT)
 Genes in the tumoural area that were associated with risk of recurrence

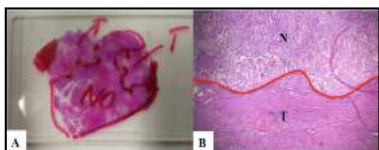
SOIL = PERITUMOUR (AT)
 Genes in the peritumoural area that were associated with risk of recurrence



CTLA4 expression in AT is associated with risk of relapse in an expanded cohort of patients

Validation set of FFPE resected tumours

(N=53)



Microscopic dissection
TT and AT



Immune profiling in AT
(770 immune-related genes)

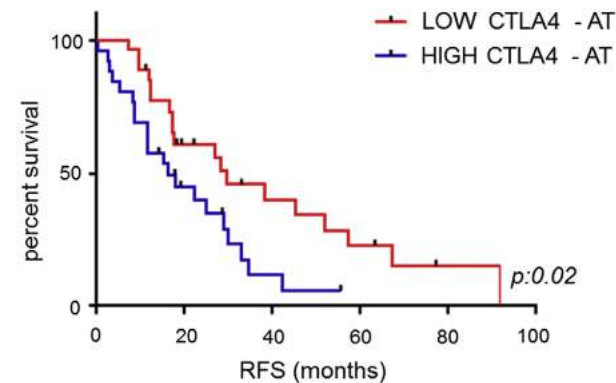
AT genes significantly related to risk of relapse at the multivariate analysis (T, N, site of tumour, R, adjuvant treatment, institution)

Adjacent Tissue				
Transcript	p-value	HR	95% CI Low	95% CI High
CCL22	0.0002	6.84	2.50	18.89
ENG	0.0001	6.30	2.45	16.25
LGALS3	0.0136	5.50	1.42	21.27
F13A1	0.0039	5.05	1.68	15.16
COLEC12	0.0056	4.80	1.58	14.53
DOCK8	0.0048	4.17	1.55	11.20
SLAMF1	0.0099	4.09	1.40	11.92
IL1R1	0.0042	4.01	1.55	10.41
LCN2	0.0166	3.95	1.28	12.17
CD209	0.0080	3.72	1.41	9.82
HLA-DQB1	0.0022	3.64	1.59	8.31
SLC11A1	0.0182	3.38	1.23	9.17
CD276	0.0077	3.25	1.37	7.75
IL2RA	0.0052	3.23	1.42	7.36
LTF	0.0086	3.13	1.34	7.34
CD200	0.0184	3.12	1.21	8.06
TLR6	0.0177	2.99	1.21	7.38
BCL2	0.0037	2.94	1.42	6.08
CKLF	0.0062	2.90	1.35	6.23
TNFRSF1B	0.0096	2.87	1.29	6.37
HLA-DMB	0.0269	2.85	1.13	7.22
RUNX1	0.0315	2.84	1.10	7.33
CARD11	0.0275	2.75	1.12	6.77
LAIR2	0.0194	2.75	1.18	6.42
CD9	0.0494	2.70	1.00	7.28
JAM3	0.0188	2.69	1.18	6.14
CTLA4	0.0191	2.65	1.17	6.00
POU2AF1	0.0146	2.59	1.21	5.57
MEF2C	0.0482	2.50	1.01	6.21
JAK3	0.0292	2.49	1.10	5.65
FCGR1A	0.0359	2.28	1.06	4.93
IL21R	0.0282	2.23	1.09	4.56
GPATCH3	0.0263	0.40	0.18	0.90
EIF2B4	0.0342	0.36	0.14	0.93
IRF1	0.0020	0.27	0.12	0.62
DEFB1	0.0003	0.21	0.09	0.49
PSMB7	0.0014	0.19	0.07	0.53
C1QBP	0.0009	0.19	0.07	0.51
CCL16	0.0169	0.18	0.04	0.73
ABCB1	0.0047	0.14	0.04	0.55
LAMP2	0.0009	0.11	0.03	0.41
IL1RAP	0.0000	0.07	0.02	0.24

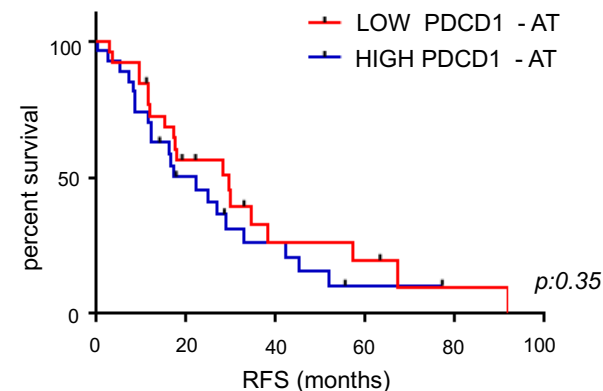
transcripts whose HIGH EXPRESSION is associated with LOWER RFS

transcripts whose LOW EXPRESSION is associated with LOWER RFS

High CTLA4 mRNA – worse prognosis

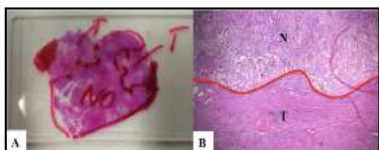


PDCD1 mRNA – no difference



CTLA4 expression in AT is associated with risk of relapse in an expanded cohort of patients

Validation set of FFPE resected tumours (N=53)



Microscopic dissection TT and AT



Immune profiling in AT (770 immune-related genes)

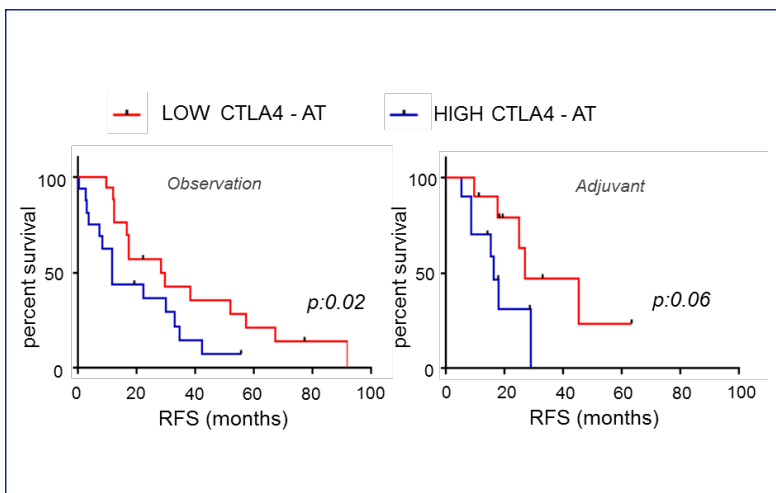
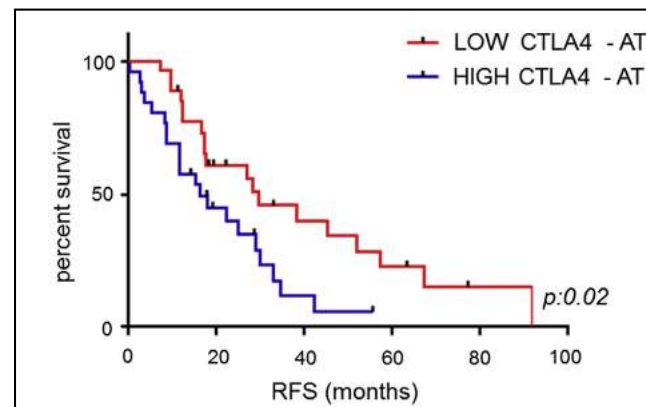
AT genes significantly related to risk of relapse at the multivariate analysis (T, N, site of tumour, R, adjuvant treatment, institution)

Adjacent Tissue				
Transcript	p-value	HR	95% CI Low	95% CI High
CCL22	0.0002	6.84	2.50	18.89
ENG	0.0001	6.30	2.45	16.25
LGALS3	0.0136	5.50	1.42	21.27
F13A1	0.0039	5.05	1.68	15.16
COLEC12	0.0056	4.80	1.58	14.53
DOCK8	0.0048	4.17	1.55	11.20
SLAMF1	0.0099	4.09	1.40	11.92
IL1R1	0.0042	4.01	1.55	10.41
LCN2	0.0168	3.95	1.28	12.17
CD209	0.0080	3.72	1.41	9.82
HLA-DQB1	0.0022	3.64	1.59	8.31
SLC11A1	0.0182	3.38	1.23	9.17
CD276	0.0077	3.25	1.37	7.75
IL2RA	0.0052	3.23	1.42	7.36
LTF	0.0086	3.13	1.34	7.34
CD200	0.0184	3.12	1.21	8.06
TLR6	0.0177	2.99	1.21	7.38
BCL2	0.0037	2.84	1.42	6.08
CKLF	0.0062	2.80	1.35	6.23
TNFRSF1B	0.0096	2.87	1.29	6.37
HLA-DMB	0.0269	2.85	1.13	7.22
RUNX1	0.0315	2.84	1.10	7.33
CARD11	0.0275	2.75	1.12	6.77
LAIR2	0.0194	2.75	1.18	6.42
CD9	0.0494	2.70	1.00	7.26
JAM3	0.0188	2.69	1.18	6.14
CTLA4	0.0191	2.65	1.17	6.00
POU2AF1	0.0148	2.59	1.21	5.57
MEF2C	0.0482	2.50	1.01	6.21
JAK3	0.0292	2.49	1.10	5.65
FCGR1A	0.0359	2.28	1.06	4.83
IL21R	0.0282	2.23	1.09	4.56
GPATCH3	0.0263	0.40	0.18	0.90
EIF2B4	0.0342	0.36	0.14	0.93
IRF1	0.0020	0.27	0.12	0.62
DEFB1	0.0003	0.21	0.09	0.49
PSMB7	0.0014	0.19	0.07	0.53
C1QB	0.0009	0.19	0.07	0.51
CCL16	0.0169	0.18	0.04	0.73
ABCB1	0.0047	0.14	0.04	0.55
LAMP2	0.0009	0.11	0.03	0.41
IL1RAP	0.0000	0.07	0.02	0.24

transcripts whose HIGH EXPRESSION is associated with LOWER RFS

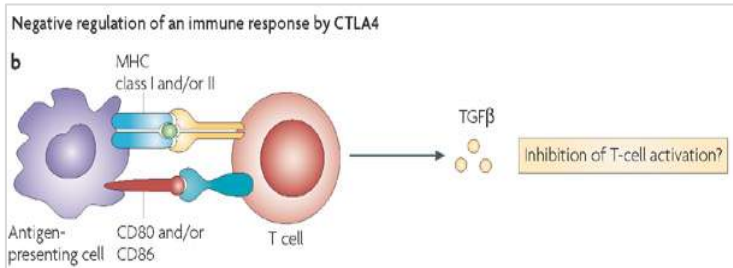
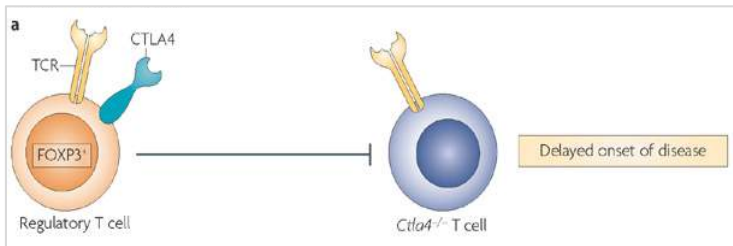
transcripts whose LOW EXPRESSION is associated with LOWER RFS

High CTLA4 mRNA – worse prognosis

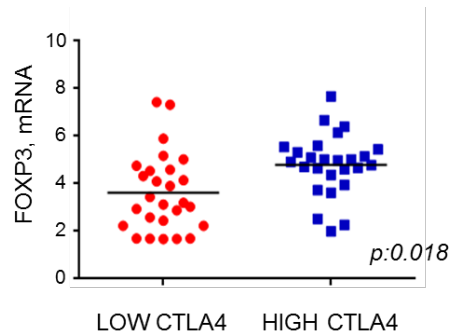


CD80 (but not CD86) expression in AT is associated with risk of relapse

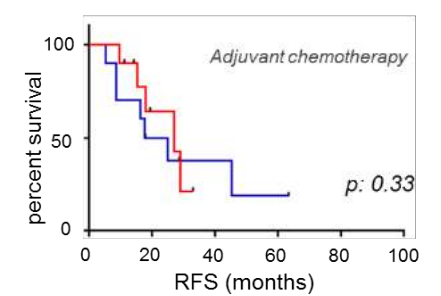
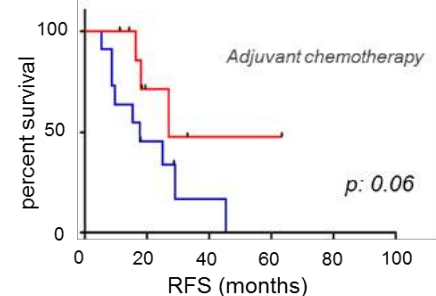
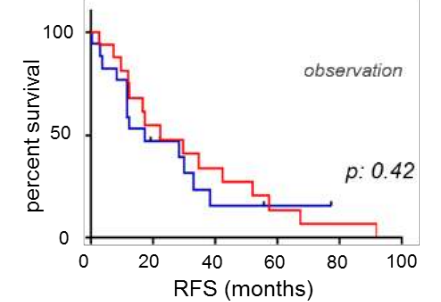
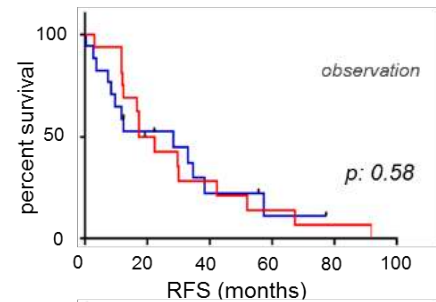
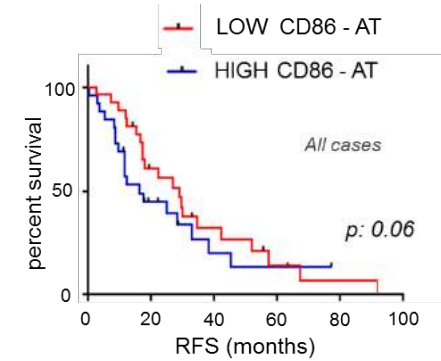
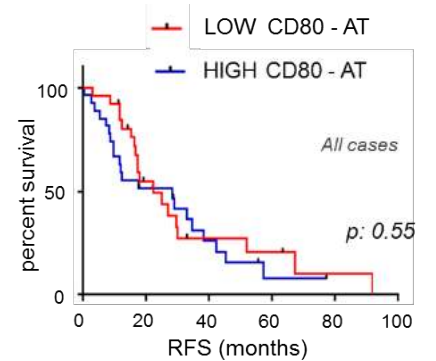
CTLA4 as a marker of Treg



Rudd E, Nat Rev Immun 2008



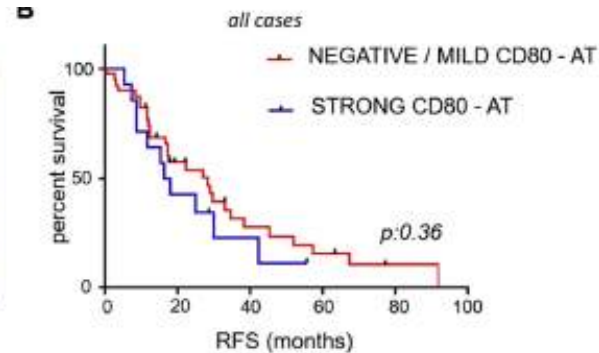
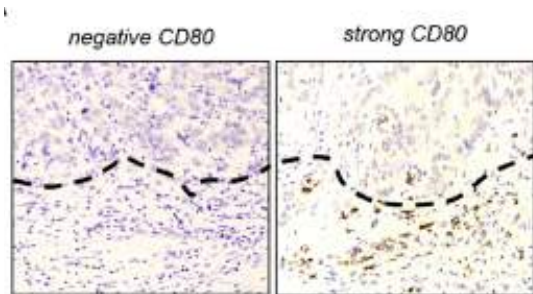
CD80 mRNA is prognostic in patients receiving adjuvant chemotherapy



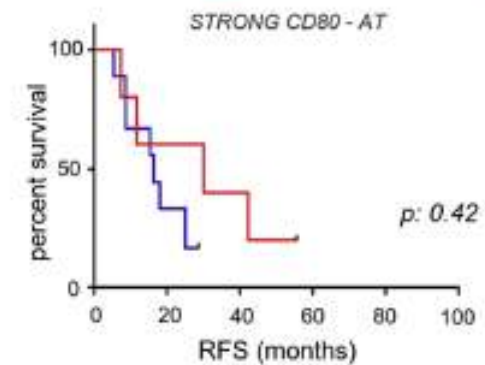
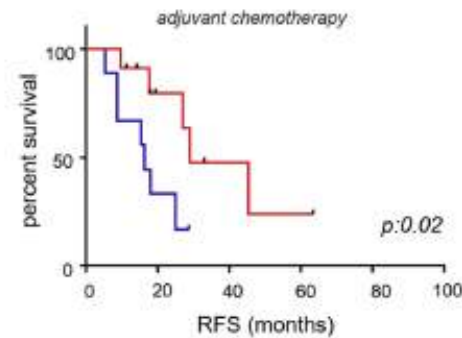
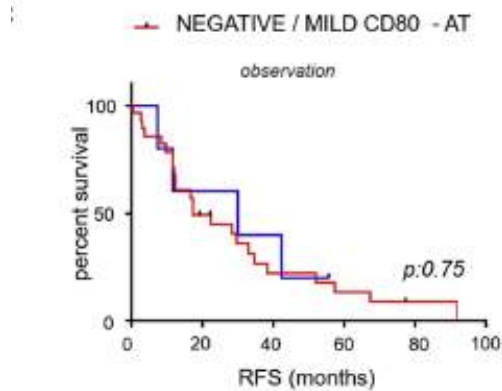
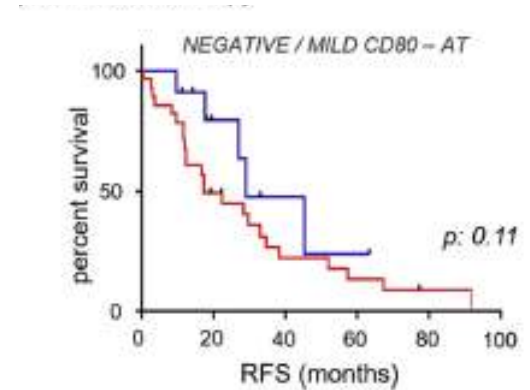
CD80 may represent a predictive biomarker of response to adjuvant treatment

CD80 protein expression is associated to better prognosis in patients receiving adjuvant treatment

Benefit from adjuvant treatment seems to be absent in case of strong CD80 expression



— observation — adjuvant chemotherapy



Immuno-related parameters affect prognosis / chemosensitivity



Exploratory set of ABC (N=123)

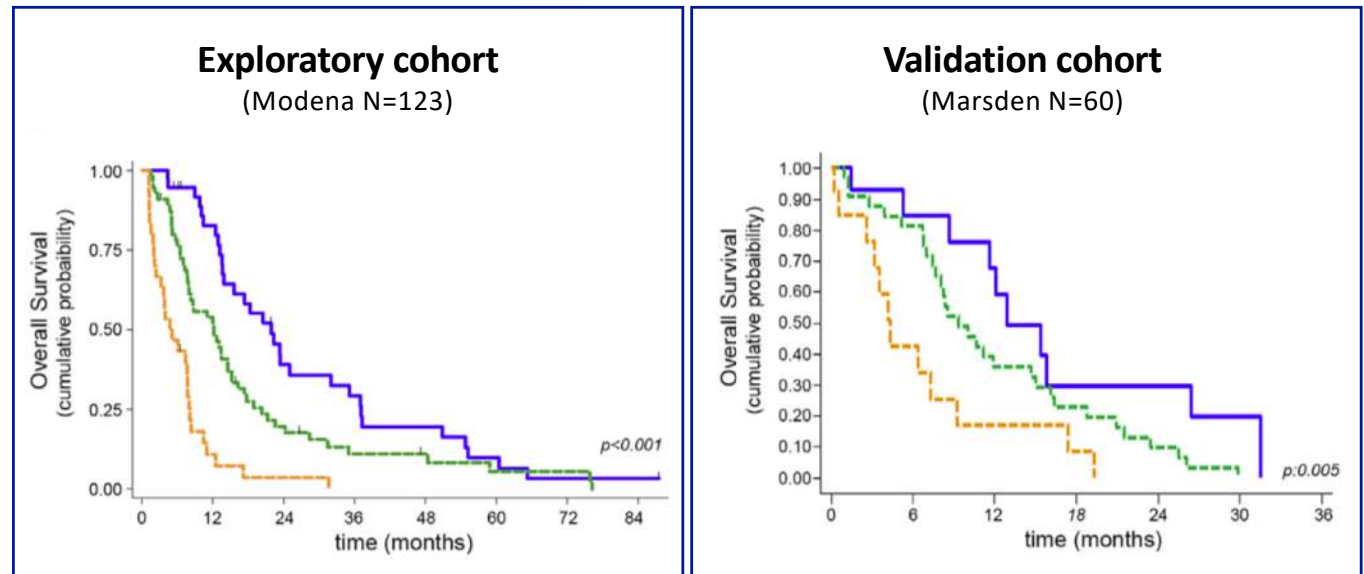
Multivariate analysis in the exploratory cohort.			
Covariate	HR	95% CI	p value
LMR			
<2.1	1.60	1.02–3.08	0.045
Albumin g/dl			
<3.5	1.62	1.04–2.50	0.031
NLR			
>3	1.74	1.03–2.97	0.042
ANC			
>8000	2.12	1.27–3.54	0.004
Performance status			
ECOG ≥2 versus 0-1	2.16	1.28–3.64	0.004
Disease status			
Metastatic versus LA	2.22	1.30–3.78	0.003
CEA ng/ml			
>9.5	2.59	1.55–4.32	<0.001

ECOG, Eastern Cooperative Oncology Group; NLR, neutrophil/lymphocyte ratio; LMR, lymphocyte/monocyte ratio; ANC, absolute neutrophil count; CEA, carcinoembryonic antigen; CI, confidence interval; HR, hazards ratio; LA, locally advanced
Variables that resulted statistically significant in the multivariate analysis are reported. Shrinkage (overfitting) 0.099. c-Harrell Train 0.702 Test 0.692.

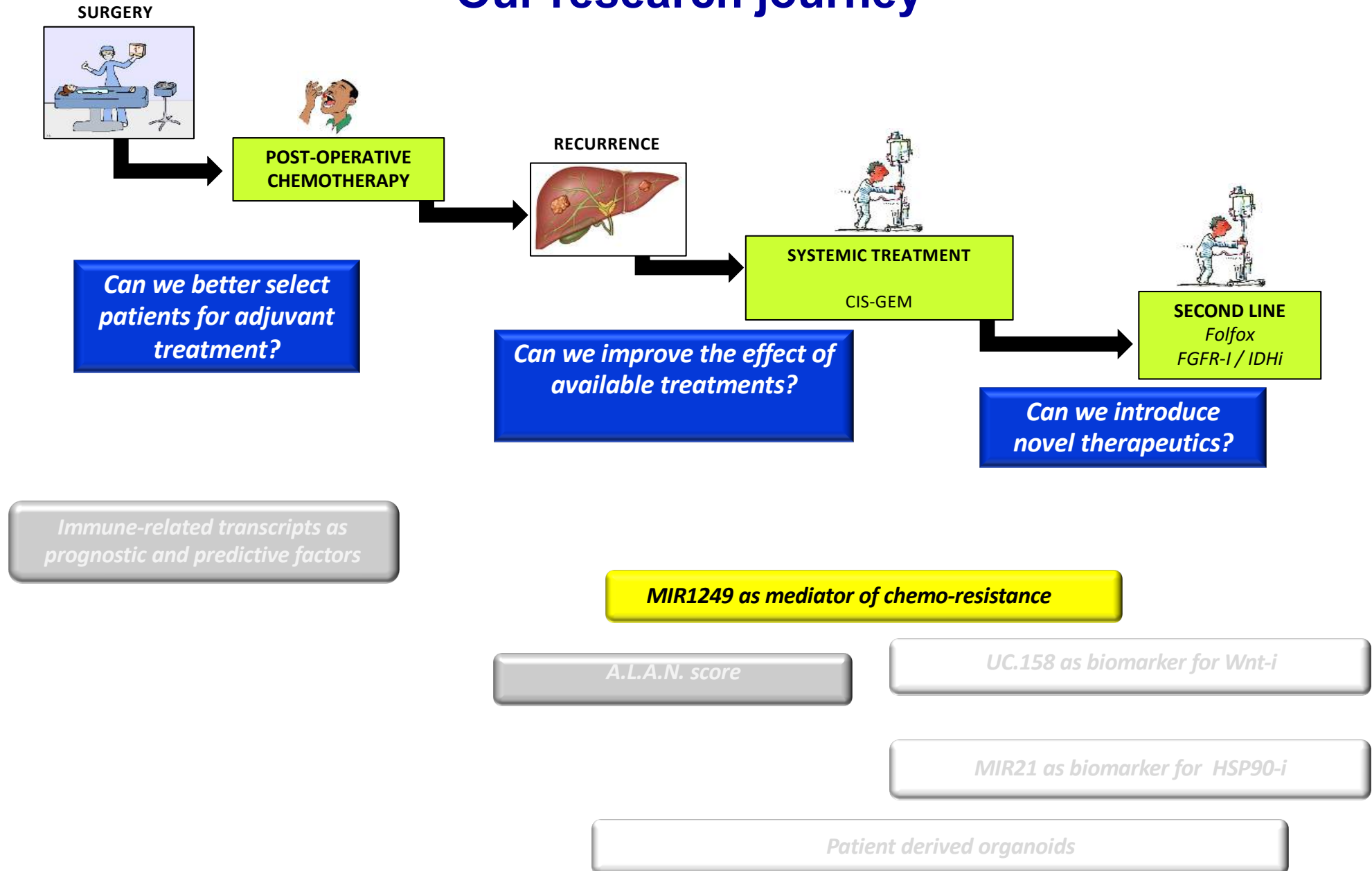
Clinical parameters associated to survival in ABC undergoing first line chemotherapy

- A** ANC – Absolute Neutrophil Count
- L** LMR – Lymphocyte Monocytes Ratio
- A** Albumin
- N** NLR – Neutrophil Lymphocytes Ratio

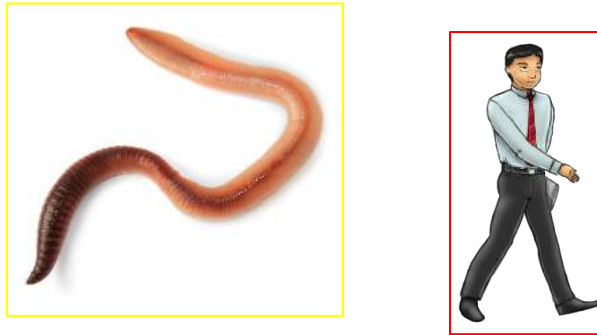
— A.L.A.N. low risk
— A.L.A.N. intermediate risk
— A.L.A.N. high risk



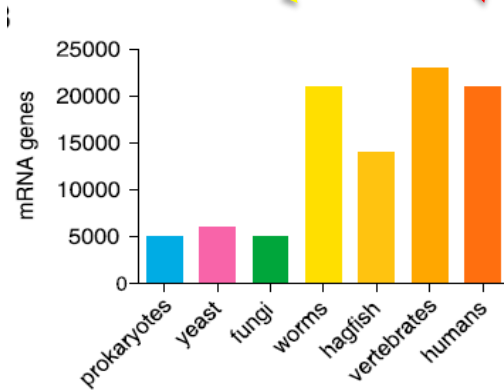
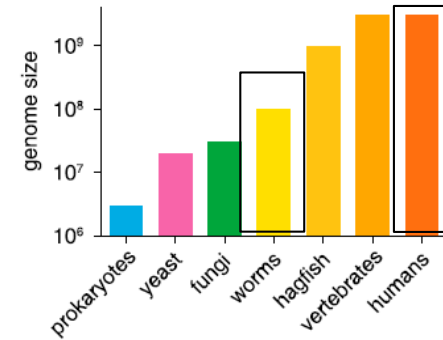
Our research journey



Is non coding RNA important?

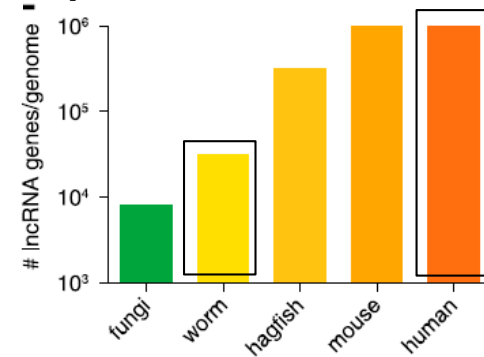


The human genome is 30 times larger than the worm genome



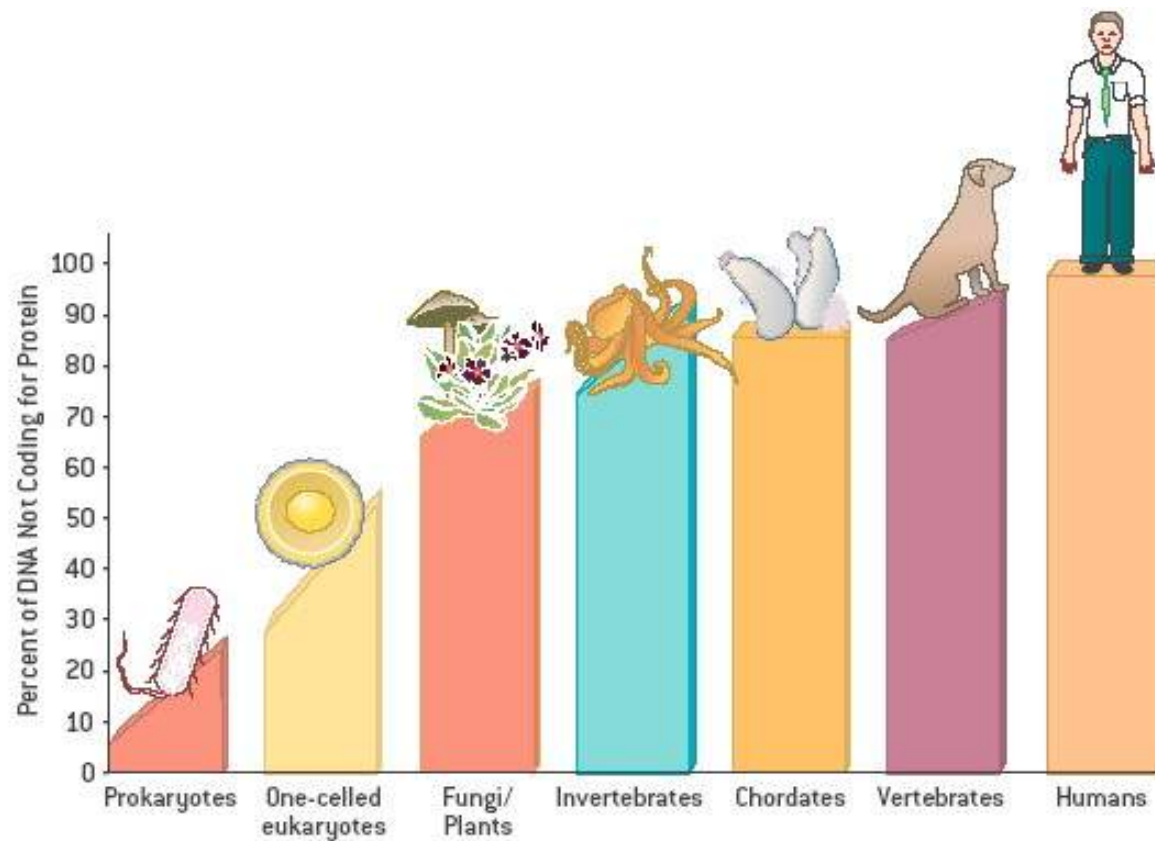
Worms and humans share the same number of protein coding mRNAs (20,000)

Humans and other vertebrates produce ~1 million unique ncRNA genes
Worms produce ~ 300,000 ncRNAs



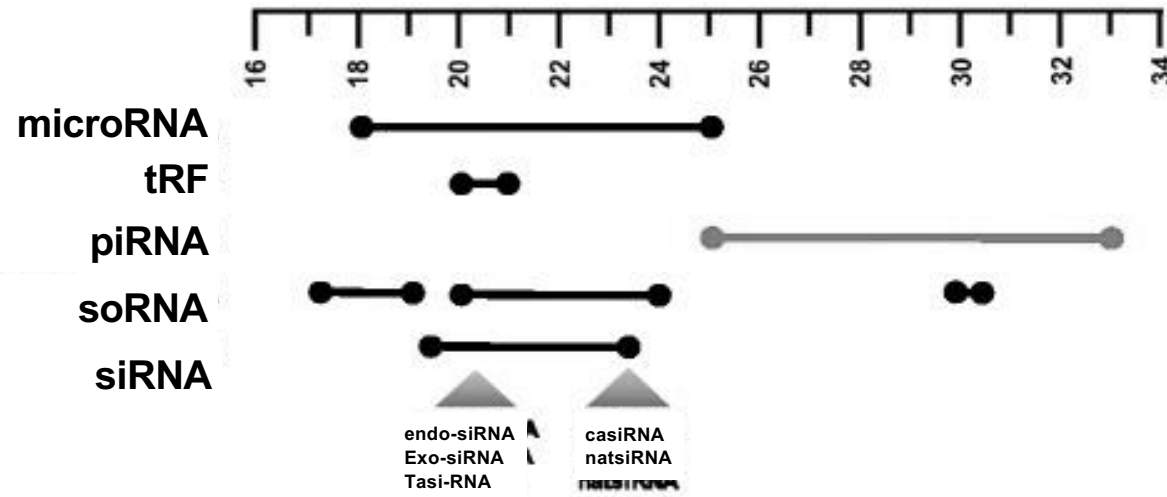
ncRNA: the master- regulator of species complexity

ncRNA has been considered “junk”, but perhaps it actually helps to explain organisms’ complexity

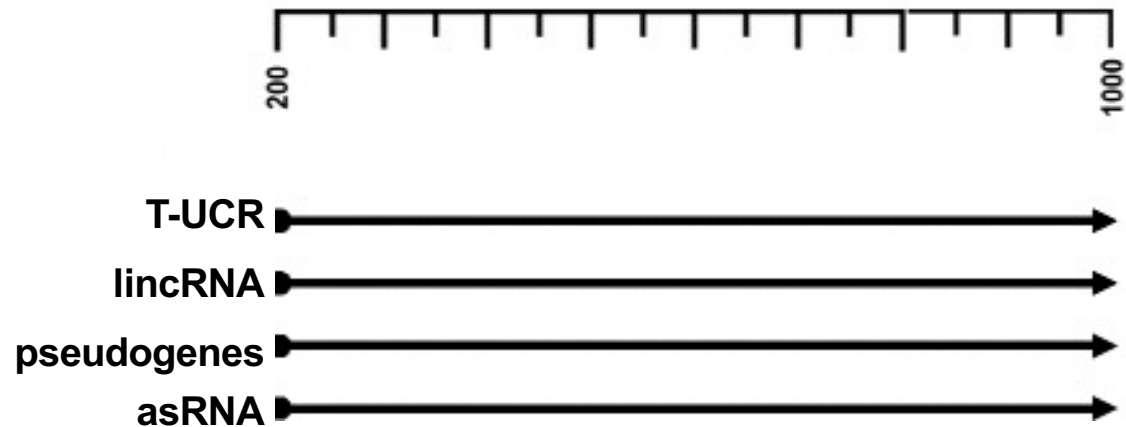


How many types of ncRNAs?

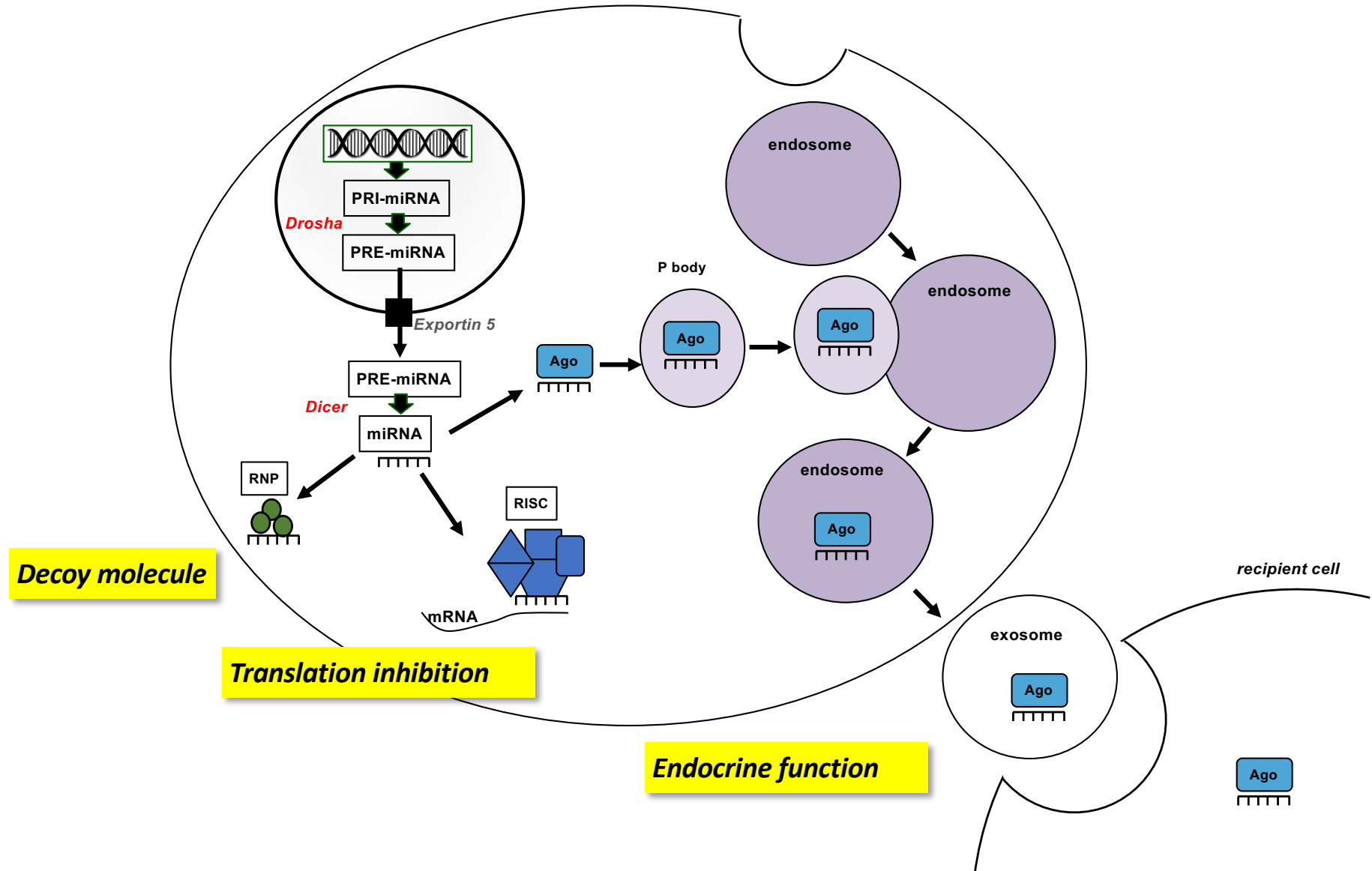
SMALL ncRNA



LONG ncRNA



How do microRNA work?



microRNA deregulation in CCA

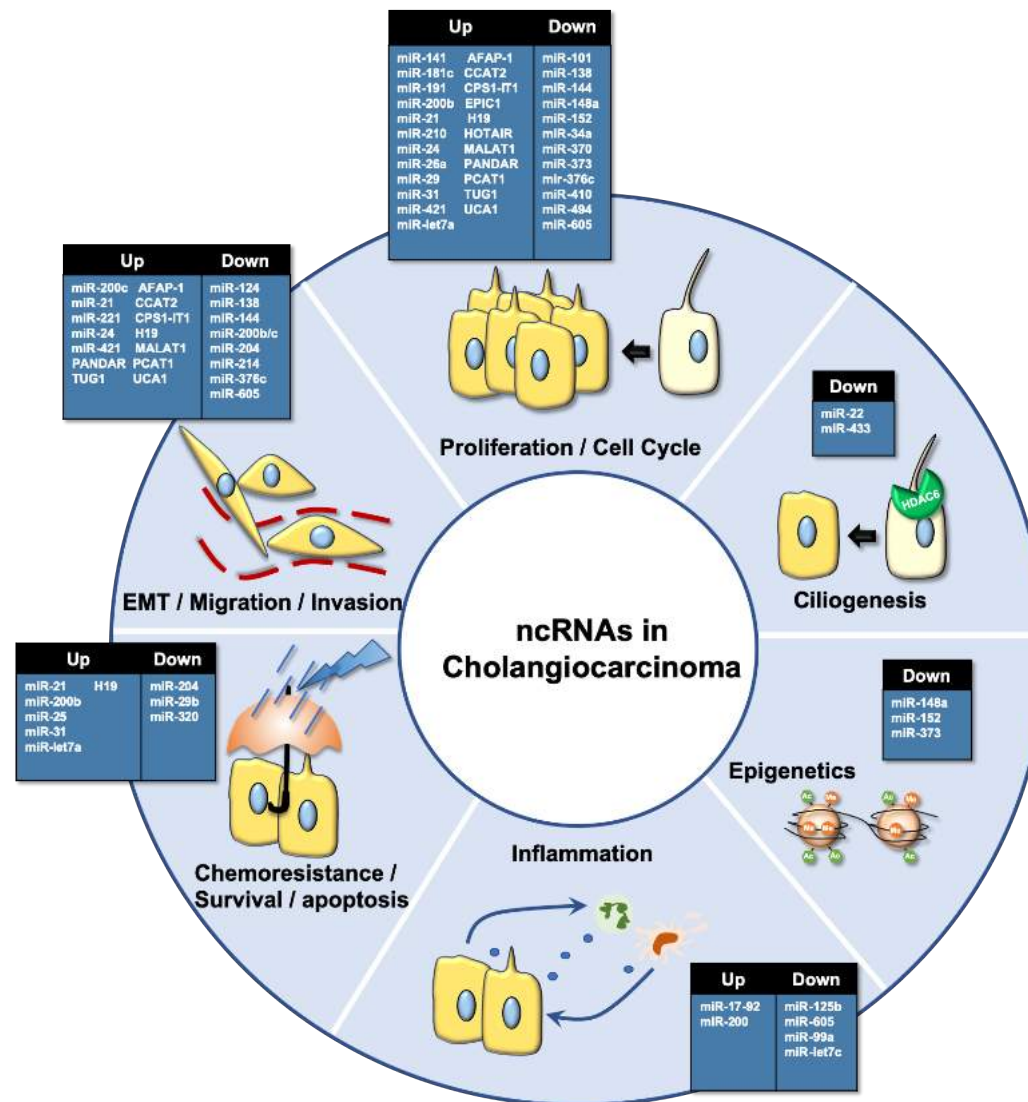
Table 1 Selected oncogenic miRNAs involved in cholangiocarcinoma initiation and progression

miRNA	Expression ^a	Tumor type	Target genes	Function	Source	Ref.
miR-21	Up	CCA, iCCA, Op-CCA	<i>PI3K, PDCD4, TIMP3, RECK, TPM1, 15PGDH, PTPN14, PTEN, KLF4, AKT, ERK</i>	Tumor growth, invasion, migration EMT,	Human cell lines, human tissue, mouse tissue	24,25,29,34,35,46
miR-25	Up	CCA	<i>DR4</i>	Antiapoptotic	Human cell lines, human tissue,	32
miR-26a	Up	CCA	<i>GSK-3β</i>	Tumor growth	Human cell lines, human tissue, mouse tissue	26
miR-31	Up	iCCA	<i>RASA1</i>	Proliferation, antiapoptotic	Human cell lines, human tissue,	27
miR-141	Up	CCA	<i>CLOCK</i>	Proliferation	Human cell lines, human tissue, mouse tissue	24
miR-210	Up	CCA	<i>MNT</i>	Proliferation	Mouse tissue	105
miR-221	Up	eCCA	<i>PTEN</i>	Invasion, migration, EMT	Human cell lines, human tissue,	37
miR-421	Up	CCA	<i>FXR</i>	Proliferation, migration	Human cell lines, human tissue	106
Let-7a	Up	CCA	<i>NF2</i>	Survival	Human cell lines, mouse tissue	42
miR-24	Up	iCCA, eCCA	<i>MEN1</i>	Proliferation, migration, angiogenesis	Human cell lines, human tissue, mouse tissue	107

Table 2 Selected oncosuppressor miRNAs in cholangiocarcinoma initiation and progression

miRNA	Expression ^a	Tumor type	Target genes	Function	Source	Ref.
miR-34a	Down	eCCA, CCA	<i>Per-1, SMAD4</i>	Proliferation, invasion, migration, EMT	Human cell lines, human tissue	103,108
miR-29b	Down	CCA	<i>Mcl1</i>	Antiapoptotic	Human cell lines	31
miR-26a	Down	CCA	<i>KRT19</i>	Suppression of tumor growth	Human cell lines, human tissue, mouse tissue	83
miR-101	Down	CCA	<i>VEGF, COX-2</i>	Angiogenesis	Human cell lines, human tissue	109
miR-124	Down	HCV-iCCA	<i>SMYD3</i>	Invasion, migration	Human cell lines,	110
miR-138	Down	CCA	<i>RhoC</i>	Proliferation, invasion, migration	Human cell lines	38
miR-144	Down	CCA	<i>LIS1</i>	Proliferation, invasion, migration	Human cell lines, human tissue, mouse tissue	111
miR-148a miR-152	Down	CCA	<i>DNMT-1</i>	Proliferation	Human cell lines, mouse tissue	44
miR-200b/c	Down	CCA, iCCA	<i>SUZ12, ROCK2, NCAM1</i>	Invasion, migration, EMT, drug resistance	Human cell lines, human tissue, mouse tissue	112
miR-204	Down	iCCA	<i>Slug, Bcl-2</i>	Invasion, migration, EMT, antiapoptotic	Human cell lines, human tissue	91
miR-214	Down	iCCA	<i>Twist</i>	EMT	Human cell lines, human tissue	36
miR-320	Down	CCA	<i>Mcl-1</i>	Antiapoptotic	Human cell lines, human tissue	91
miR-370	Down	CCA	<i>MAP3K8, WNT10B</i>	Proliferation	Human cell lines, human tissue, mouse tissue	43,113
miR-373	Down	pCCA	<i>MBD2</i>	Proliferation	Human cell lines, human tissue	114
miR-376c	Down	iCCA	<i>GRB2</i>	Proliferation, migration	Human cell lines	115
miR-410	Down	CCA	<i>XIAP</i>	Proliferation	Human cell lines, human tissue, mouse tissue	43
miR494	Down	CCA	<i>CDK6, PLK1, PTTG1, CCNB1, CDC2, CDC20 TOP2A,</i>	Proliferation	Human cell lines, mouse tissue	30,116
let-7c/ miR-99a/ miR-125b	Down	CCA	<i>IL-6, IL-6R, IGF1R</i>	Inflammation, invasion, migration	Human cell lines, human tissue, mouse tissue	41

Multi-tasking players in cancer promotion and progression

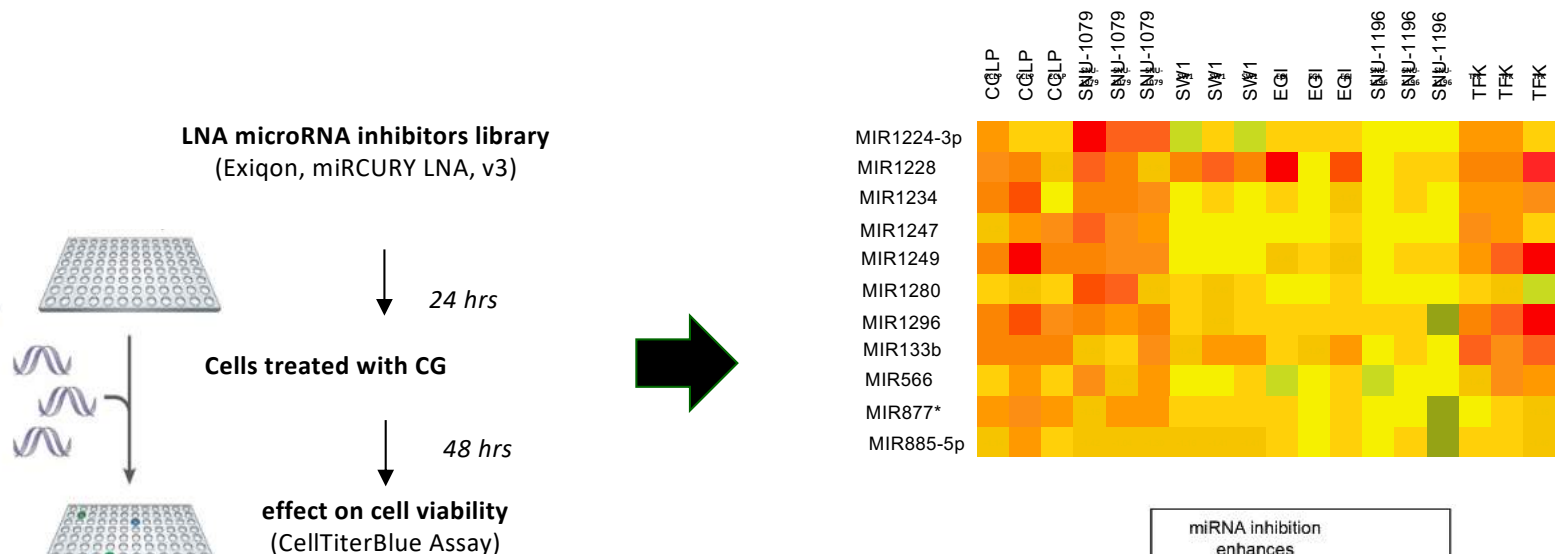




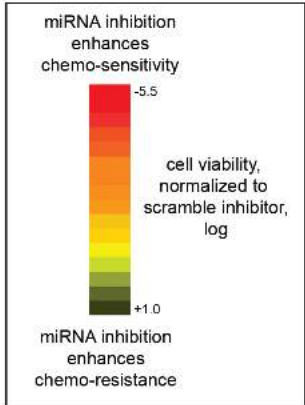
miRNAs as modulators of chemoresistance in CCA

Highthroughput screening to identify miRNA-i that reverse chemotherapy resistance in human CCA cells

Functional approach that modulates expression of miRNAs involved in cell dynamics

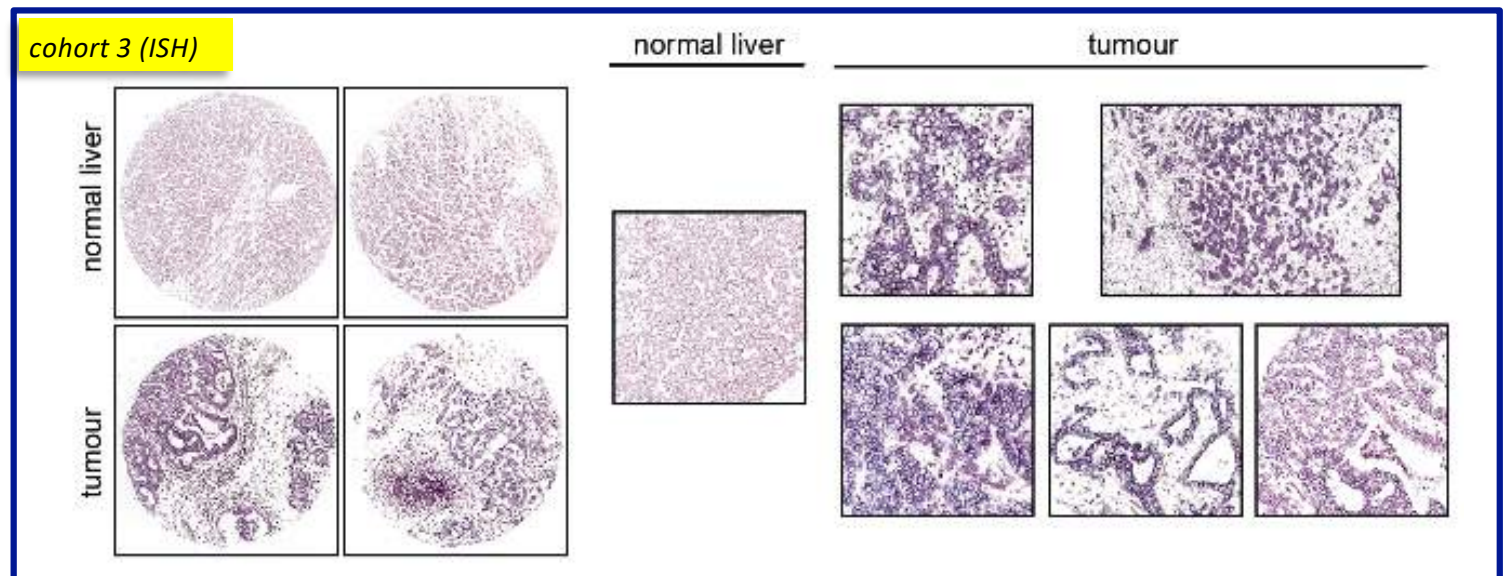
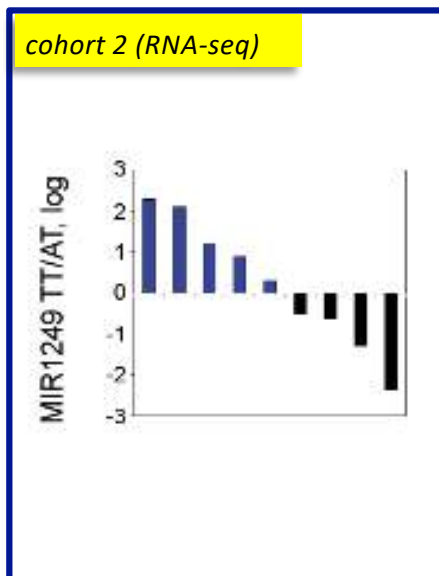
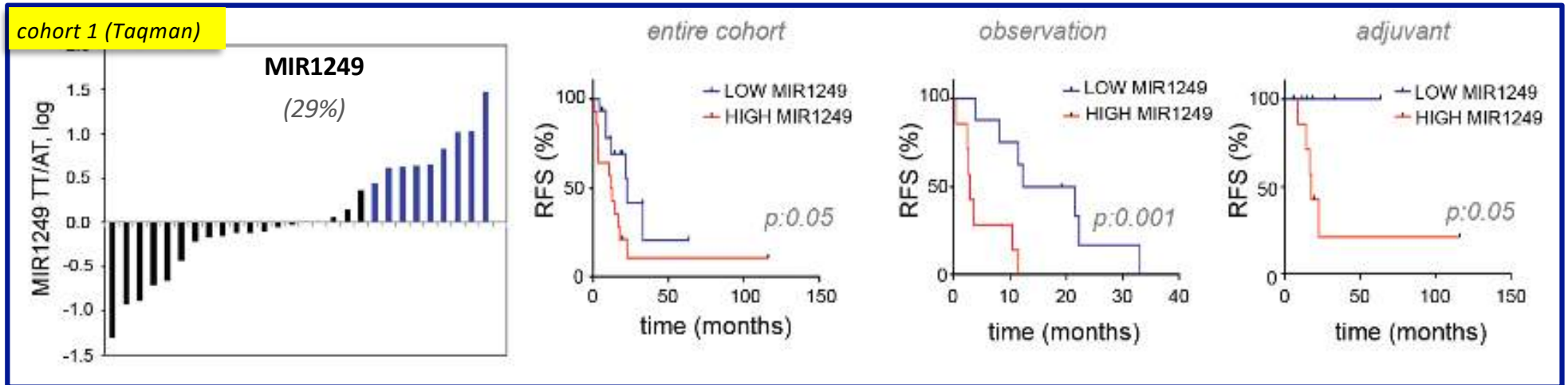


Analysis of the HTS: For each replicate: cell viability assessed for each hit normalized to averaged NEG CTRLs across the plates. For each cell line: t-test of normalized values for 3 replicates (p value < 0.05).



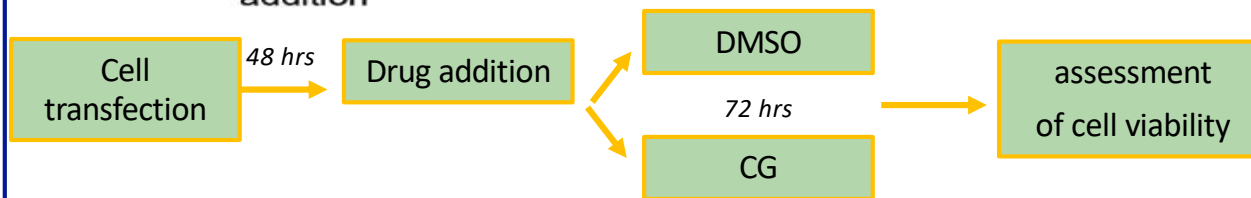
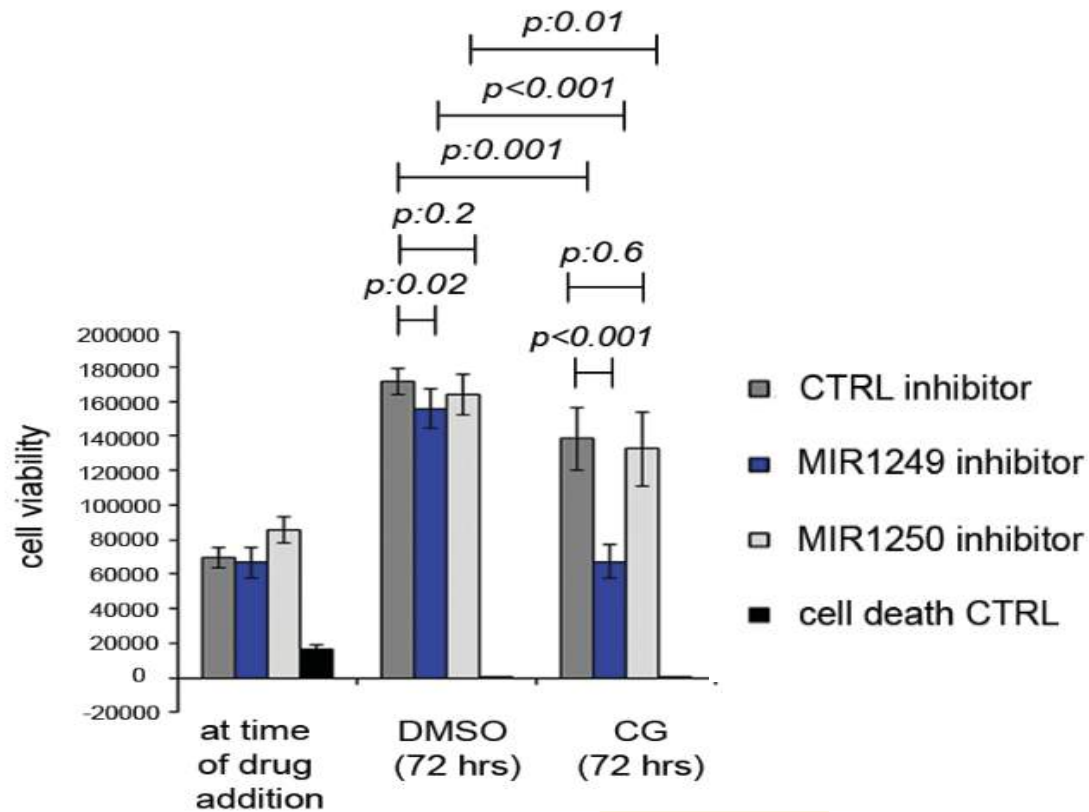
MIR1249 is clinically relevant

MIR1249 is over-expressed in 30-50% of human CCA tissues



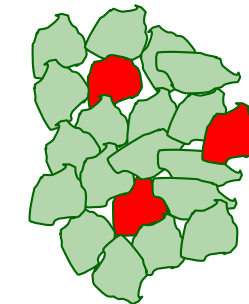
MIR1249i activity is specific for chemotherapy treatment

MIR1249i decreases cell viability only in CG-treated cells

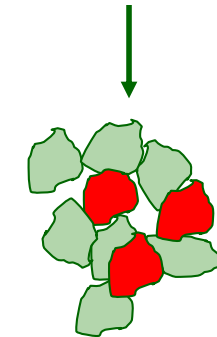


Hypothesis:

MIR1249 drives survival and growth of chemo-resistant cells



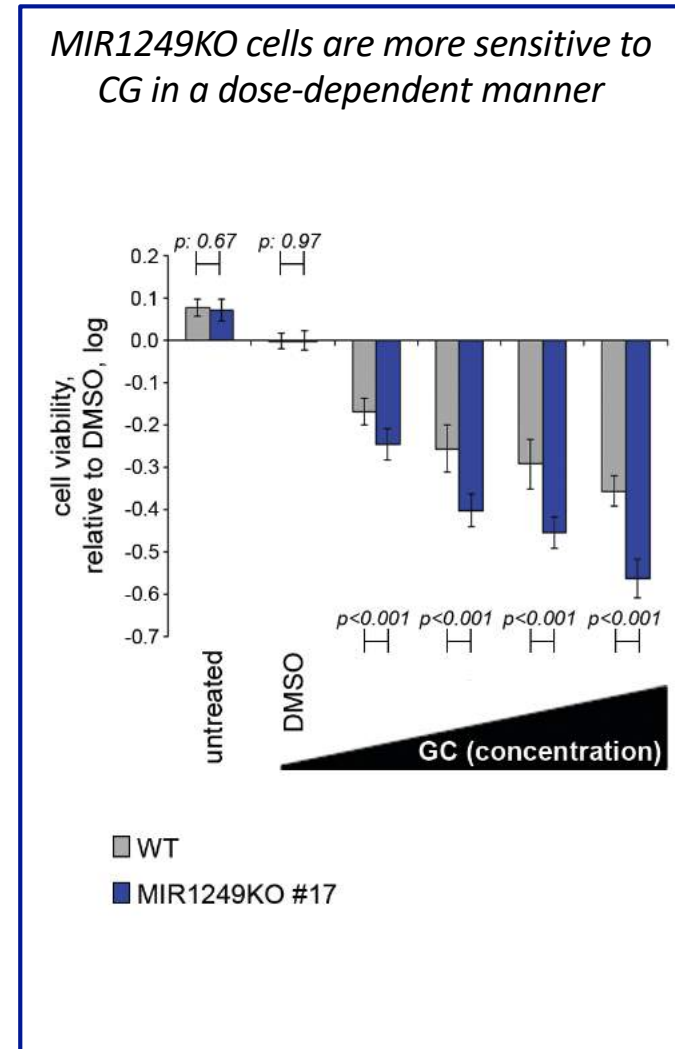
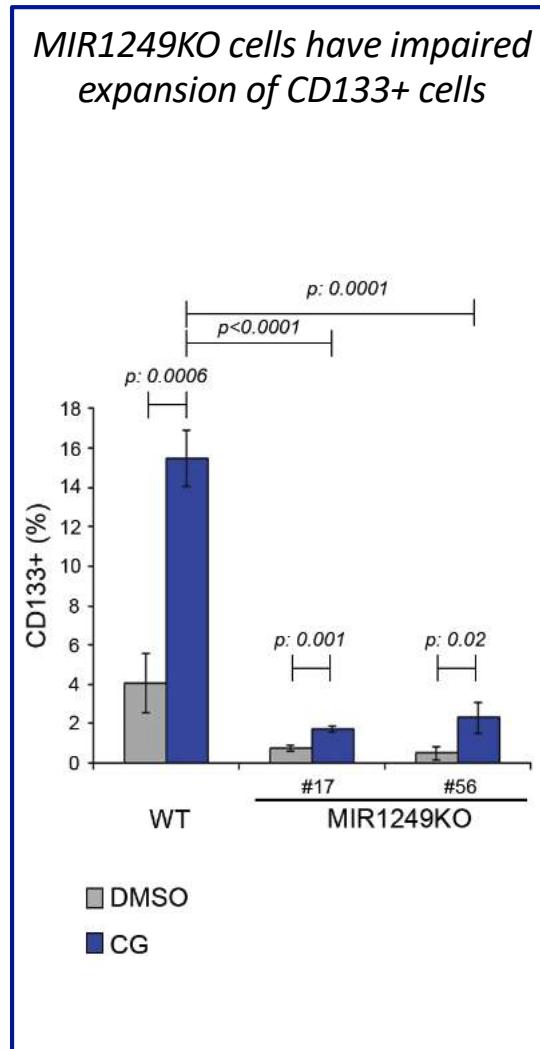
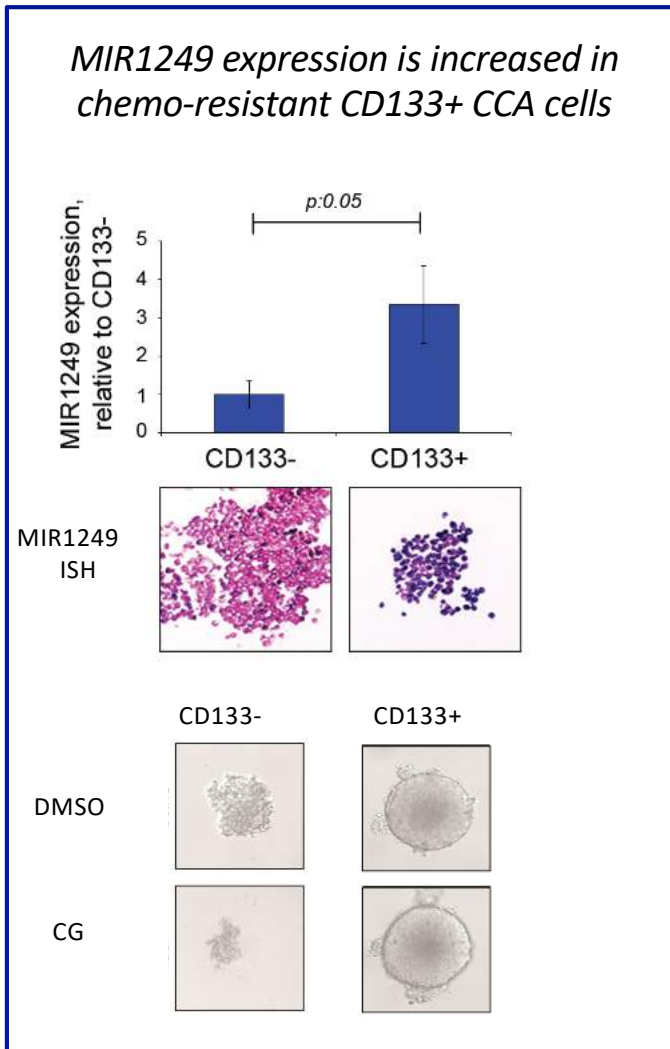
chemotherapy



Enrichment of resistant cells

MIR1249 drives expansion of CD133+ cells

MIR1249 inhibition sensitizes CCA cells to CG chemotherapy by reducing expansion of CD133+ cells

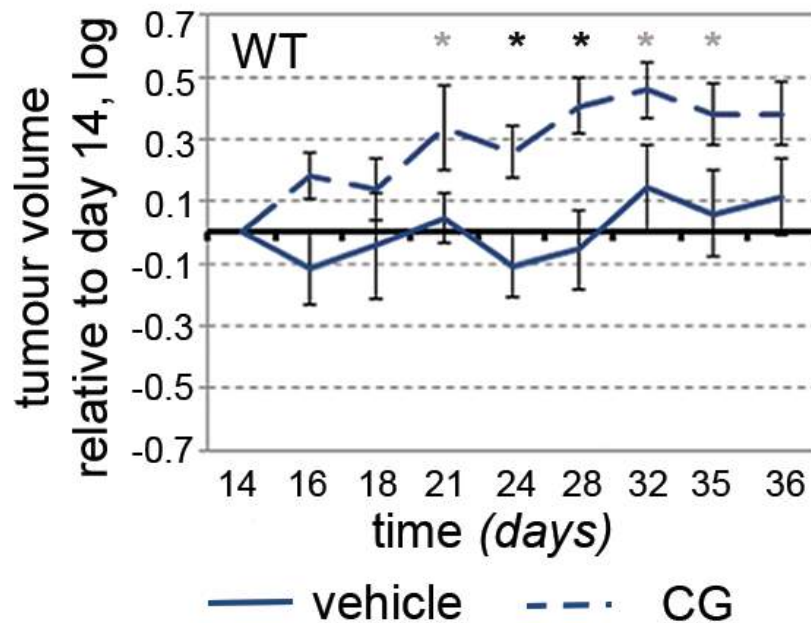




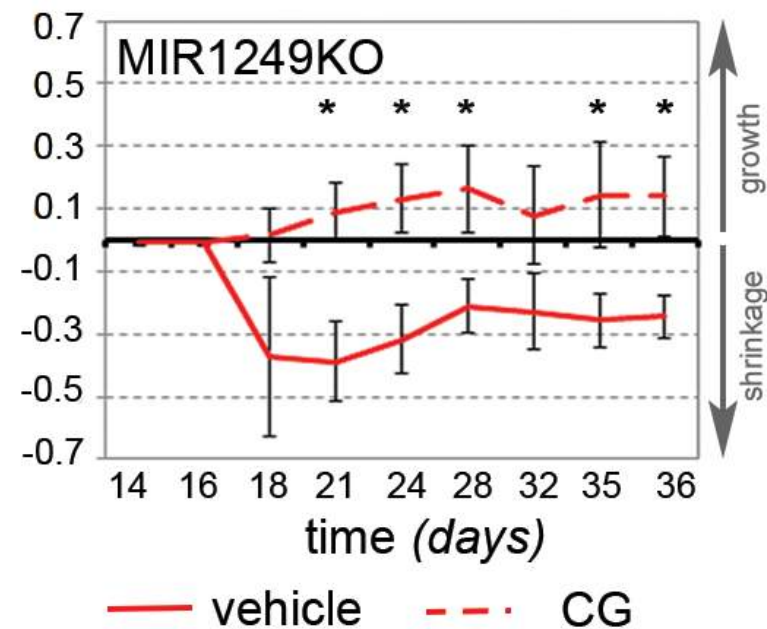
MIR1249i induces tumour response *in vivo*

CG chemotherapy sensitivity is enhanced in MIR1249KO mice xenografts

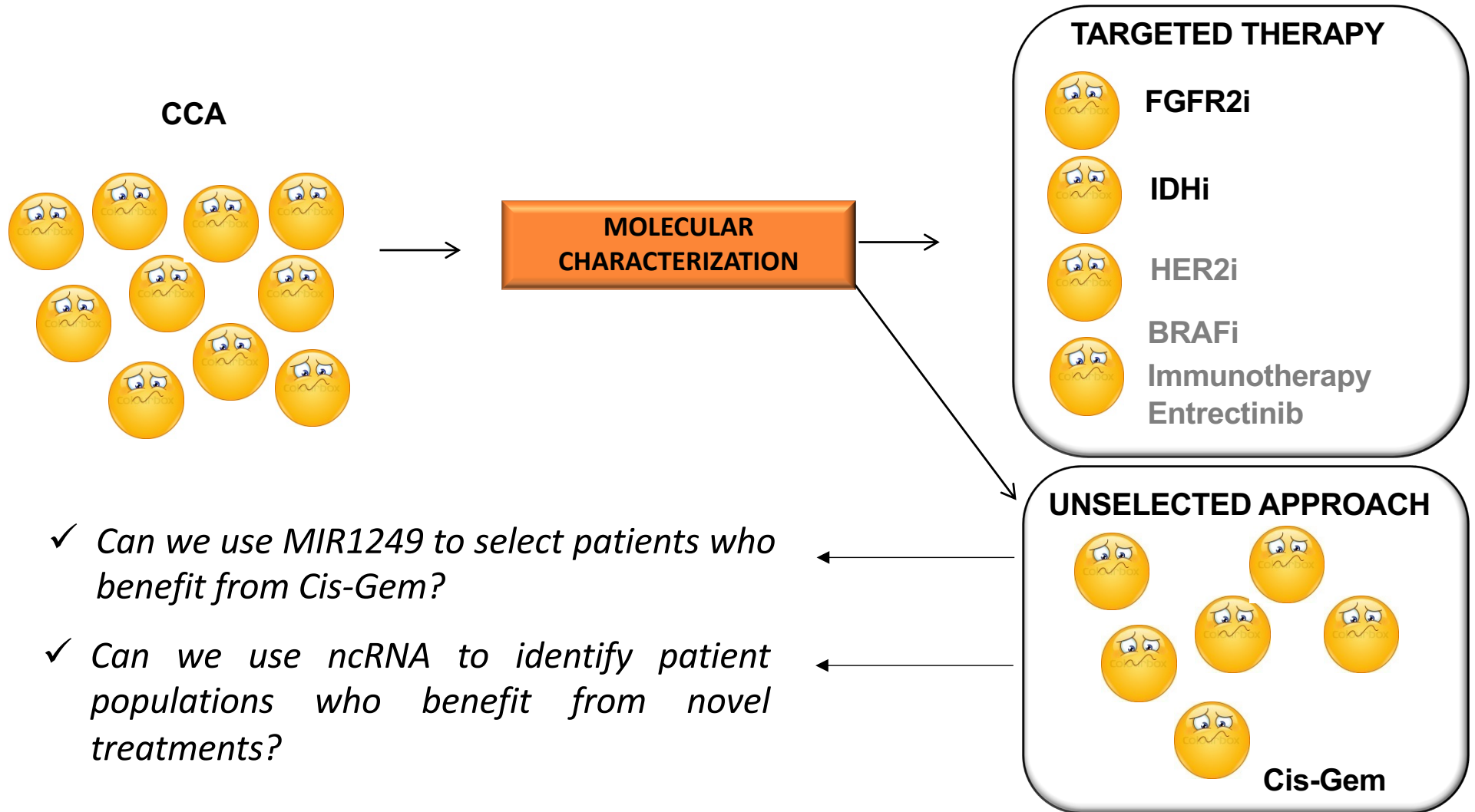
CG induces stabilization of disease in WT



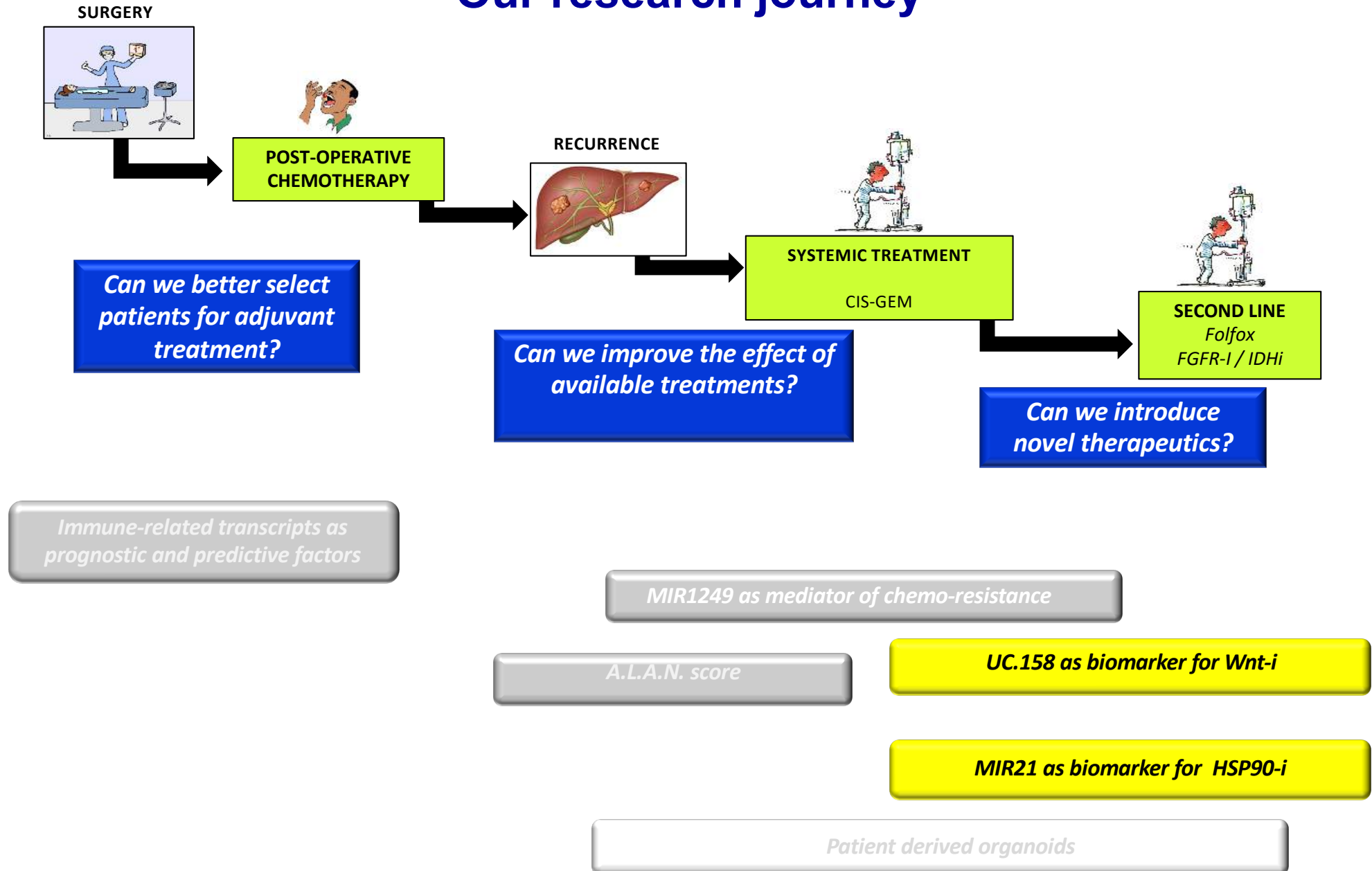
CG induces tumour shrinkage in animal models with lack of MIR1249



Expanding precision oncology beyond mutational status



Our research journey

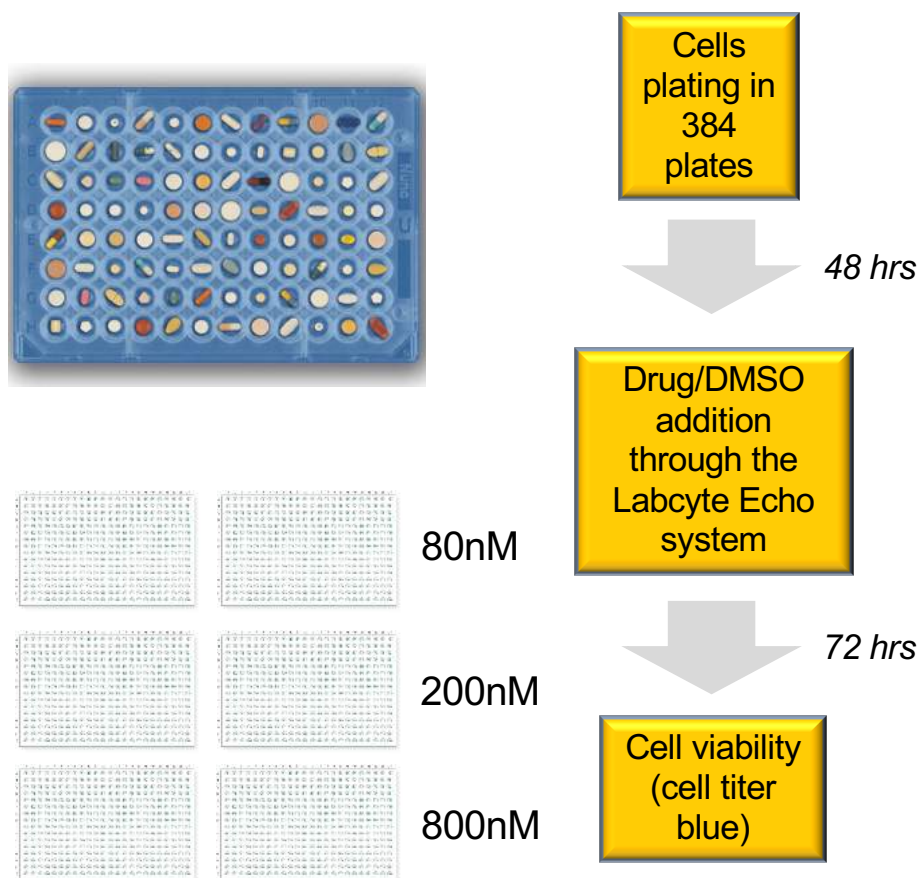


Our experience of integration of non coding RNAs and organoid models in drug discovery projects in CCA



Preclinical testing of small molecule drugs in CCA disease model (cell lines)

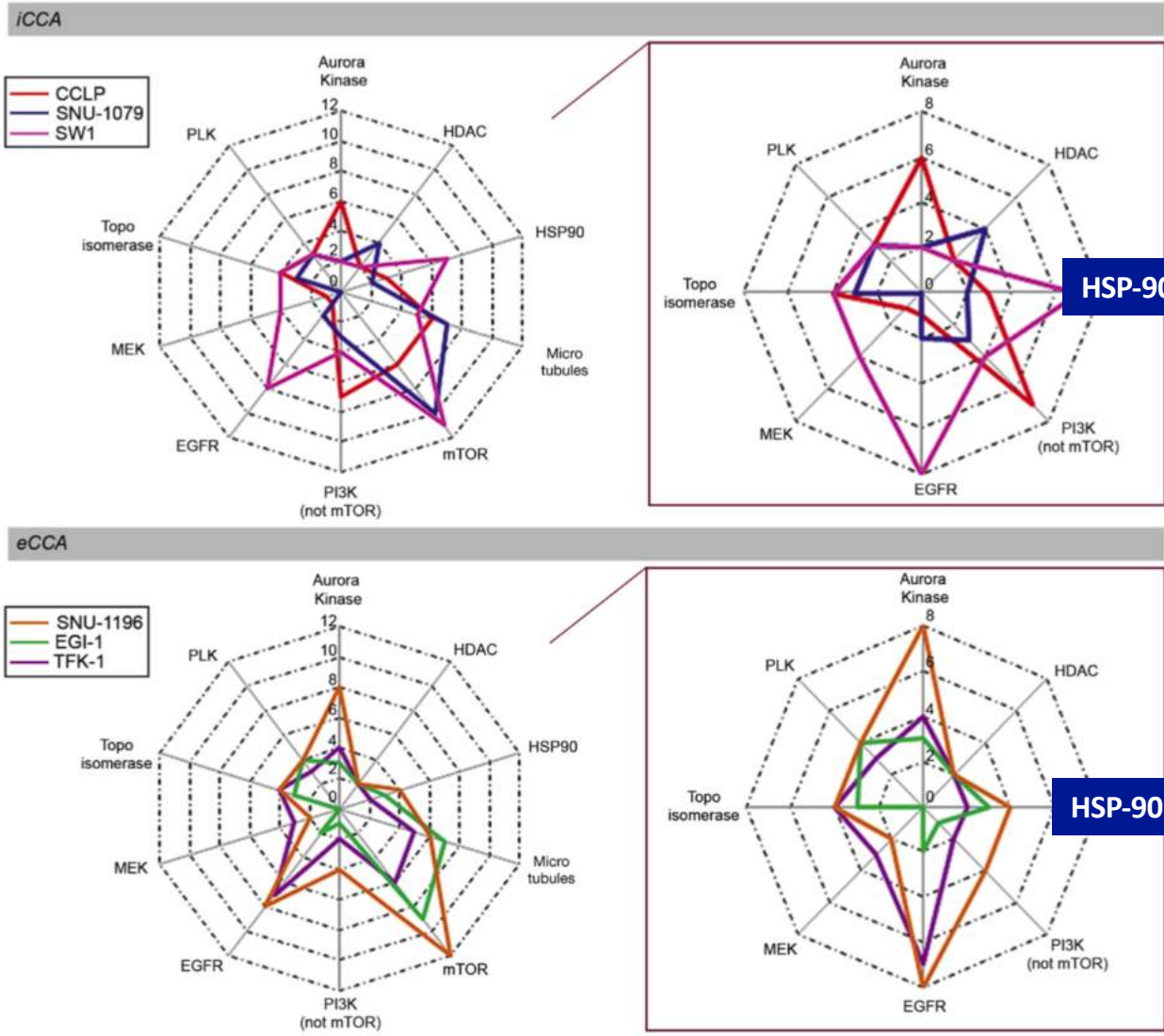
Highthroughput screening of small molecule compounds (n=500)



CCA cell lines

Cell line	Tumour type	Origin	Mutations
EGI-1	ECC	Extrahepatic bile ducts	TP53
TFK-1	ECC	Middle common bile duct	BAP1 PBRM1
Snu-1196	ECC	Hepatic duct bifurcation	SMAD4 TP53
Snu-245	ECC	Distal common bile duct	KRAS TP53
Snu-869	ECC	Ampulla of Vater	TP53
Snu-478	ECC	Ampulla of Vater	MLH1 TP53
Witt (MzCh-A)	GBC	Adenocarcinoma of Gallbladder	SMAD4 TP53
Snu-308	GBC	Adenocarcinoma of Gallbladder	TP53
SW1	ICC	Intrahepatic cholangiocarcinoma	-
CC-LP	ICC	Intrahepatic cholangiocarcinoma	BAP1
Snu-1079	ICC	Intrahepatic cholangiocarcinoma	IDH1 PBRM1

Enrichment pathway analysis identifies therapeutic opportunities for CCA



Enrichment for microtubule associated drugs and mTOR inhibitors in all cell lines.

Clinical trials are ongoing for these compounds.

Enrichment of HDAC inhibitors for Snu-1079 that harbours mutations in IDH1 and PBRM1 chromatin remodeling genes.

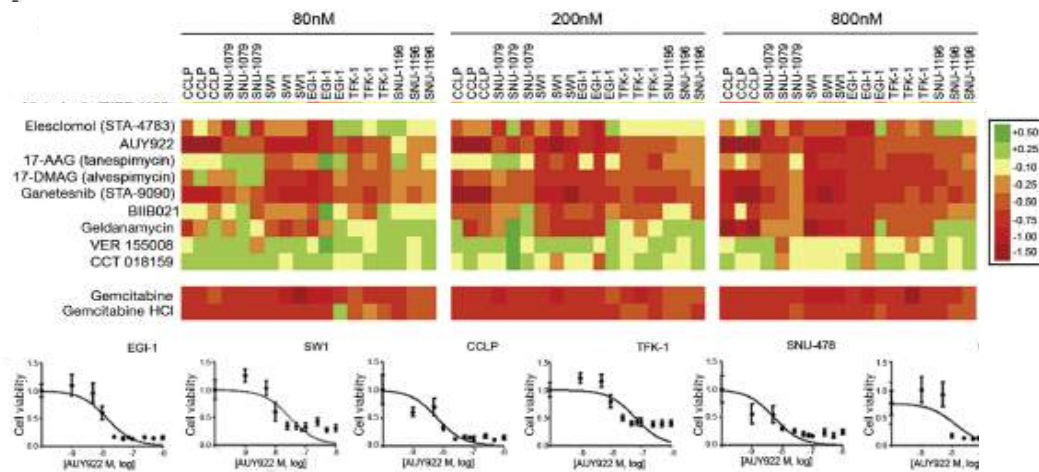
in line with previous observations (Chao, Nature. 2012)

Heat Shock Protein (HSP) 90 inhibitors were effective in all cell lines

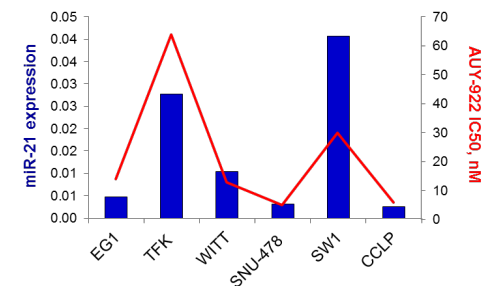
HSP-90 inhibition has recently proved effective in CCA preclinical models (Shirota, Mol Cancer Ther. 2015)

HSP90i is effective and its activity is increased by lack of MIR21 expression in human CCA cell lines

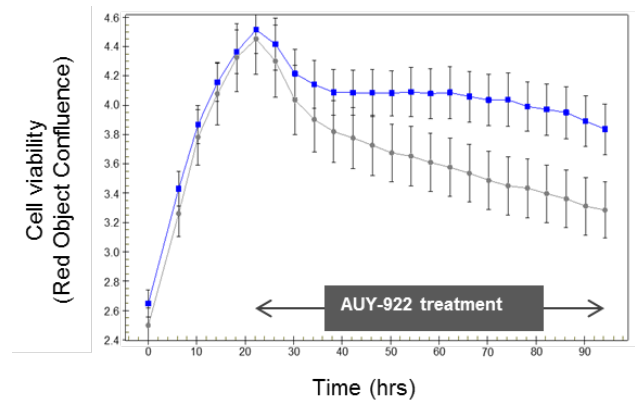
Highthroughput screening of small molecule compounds (n=500) identifies HSP90-i as effective drugs in human CCA cell lines



Response to HSP90-i is inversely related to MIR21 expression

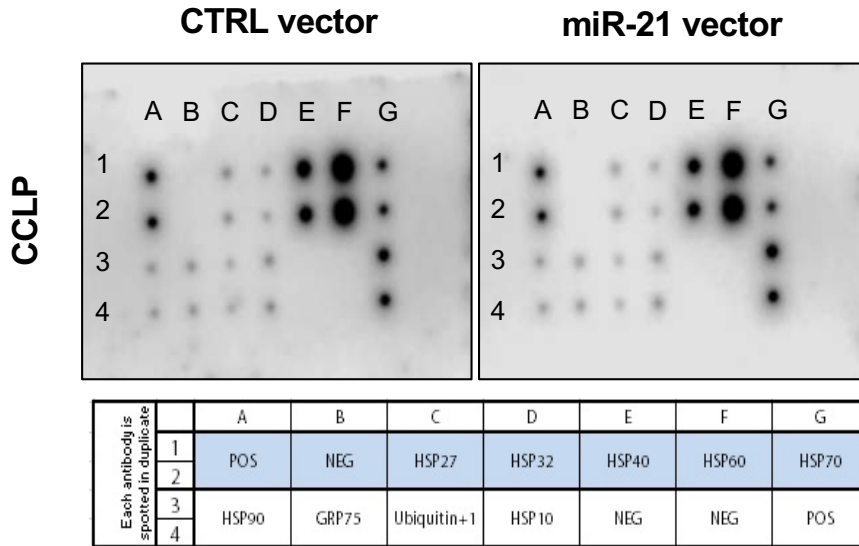


MIR21 inhibition increases sensitivity to HSP90-i

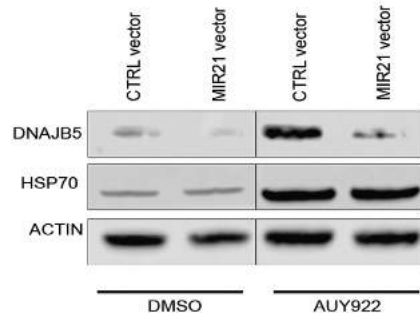


miR-21 can target DNAJ5B mRNA

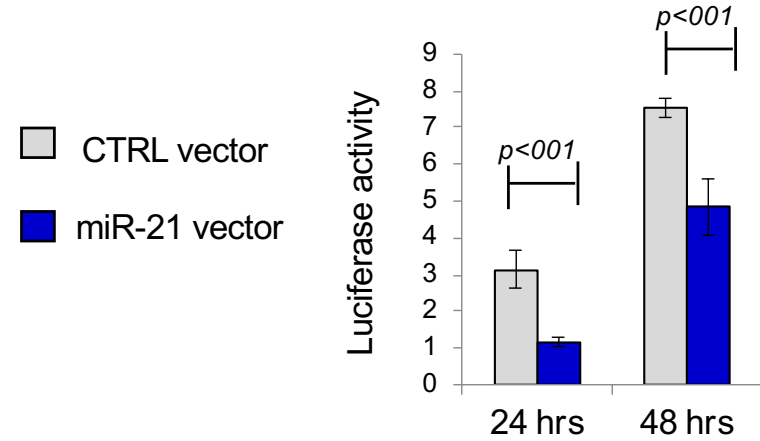
HSP protein array in CCLP cells over-expressing miR-21



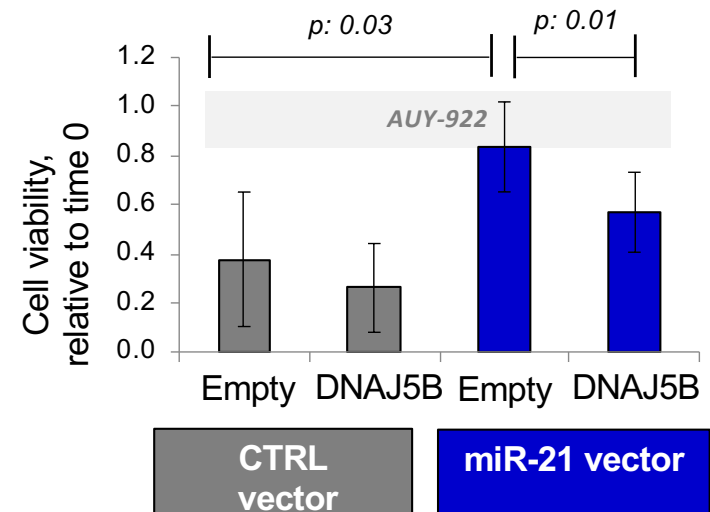
DNAJ5B protein expression reduces after miR-21 expression



Luciferase assay confirms direct binding between miR-21 and DNAJ5B 3'UTR



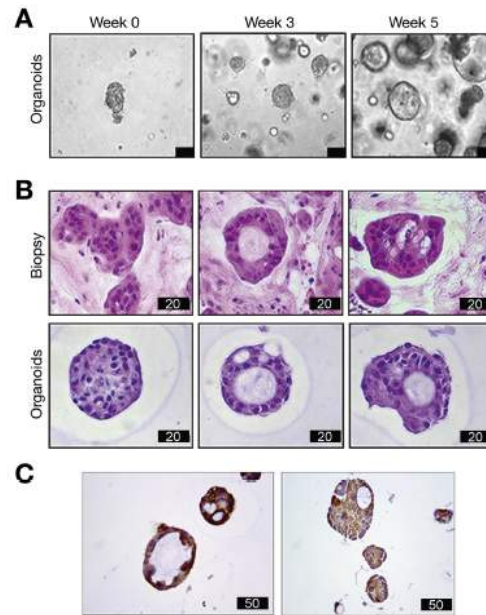
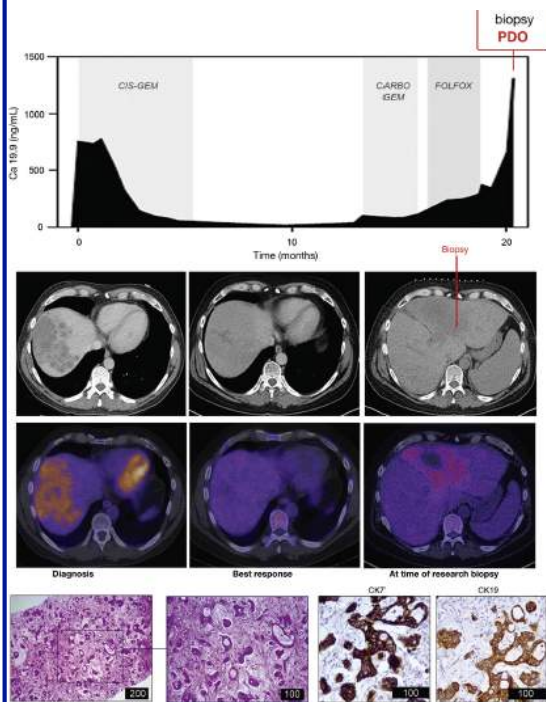
Co-transfection of miR-21 and DNAJ5B rescues biological effect



MIR21-dependent HSP90i activity has been confirmed in patient's derived preclinical models

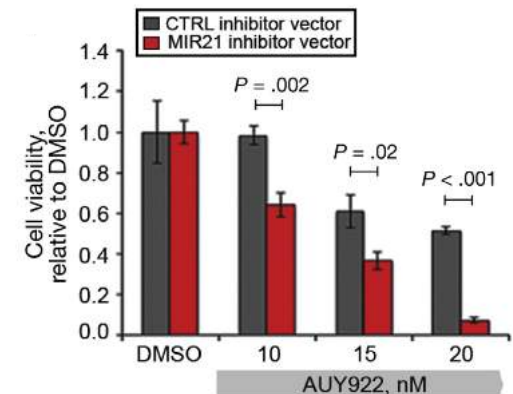
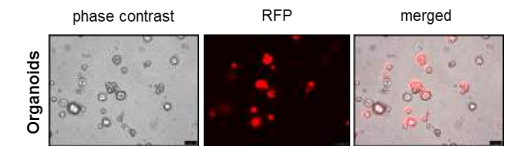


Patients derived organoids were established from chemo-refractory CCA patients



HSP90-i remains effective in CCA organoids, but its activity was significantly increased by MIR21 silencing

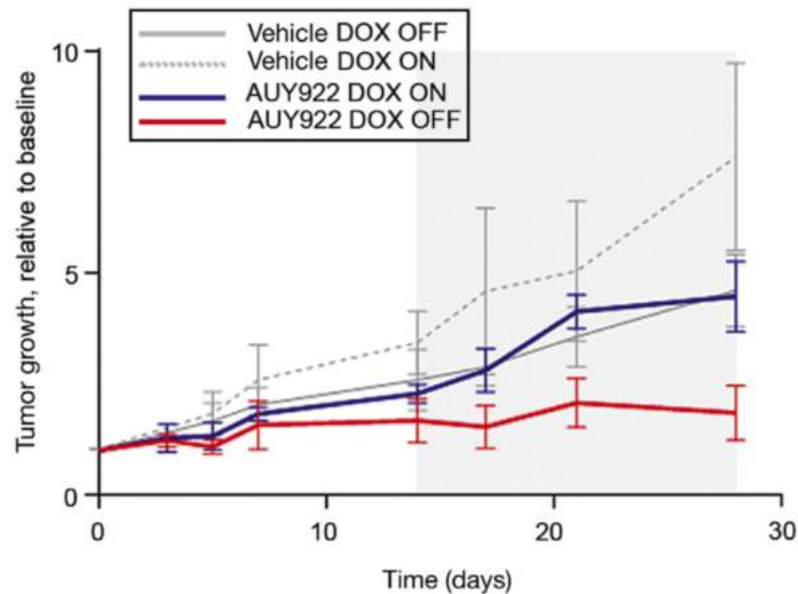
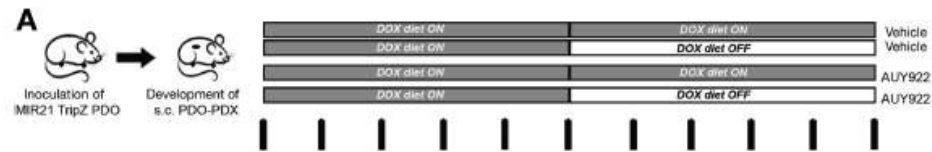
- Nilotinib
- Crizotinib
- XL147
- Afatinib
- Erlotinib
- AUY922
- NVP-TAE684
- Everolimus
- Bortezomib
- Gefitinib
- Brivanib
- Imatinib
- Olaparib
- SGX-523
- Sorafenib
- GSK690693
- Saracatinib
- Selumetinib
- MK-2206
- Linsitinib
- Palbociclib
- Dasatinib
- Tandutinib
- OSI-930
- Regorafenib
- Oxaliplatin
- ENMD-2076
- Tivozanib
- 5-FU
- Vemurafenib
- Barasertib
- AZD6482
- AZD7762
- Erismodegib
- KU-60019
- Rigosertib
- MK-1775
- Lapatinib
- CP-466722
- LY2157239
- GDC-0980
- Dacomitinib
- Irinotecan
- Trametinib
- Ruxolitinib
- LY2109761
- Torin 2
- CHIR-99021
- FR-180204
- LGK-974
- SCH772984
- SB265610
- CCT251455
- CCT252422
- CCT241736



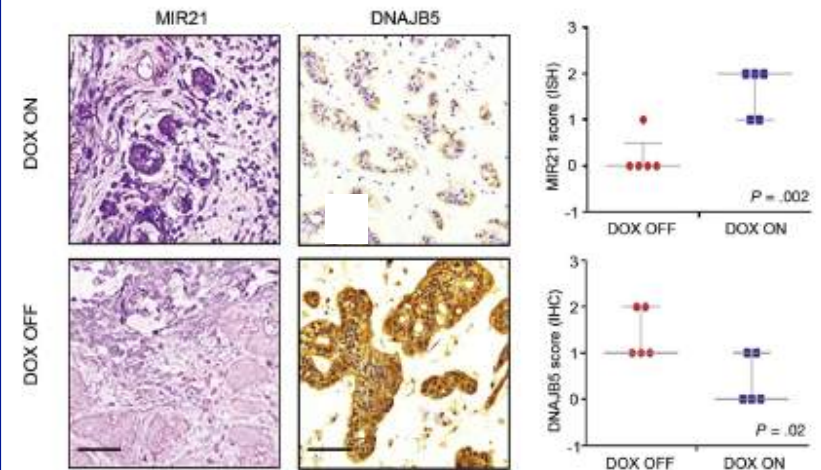
Modulation of MIR21 in vivo controls HSP90i efficacy

PDO-derived PDX confirmed dependence of HSP0-i efficacy on MIR21

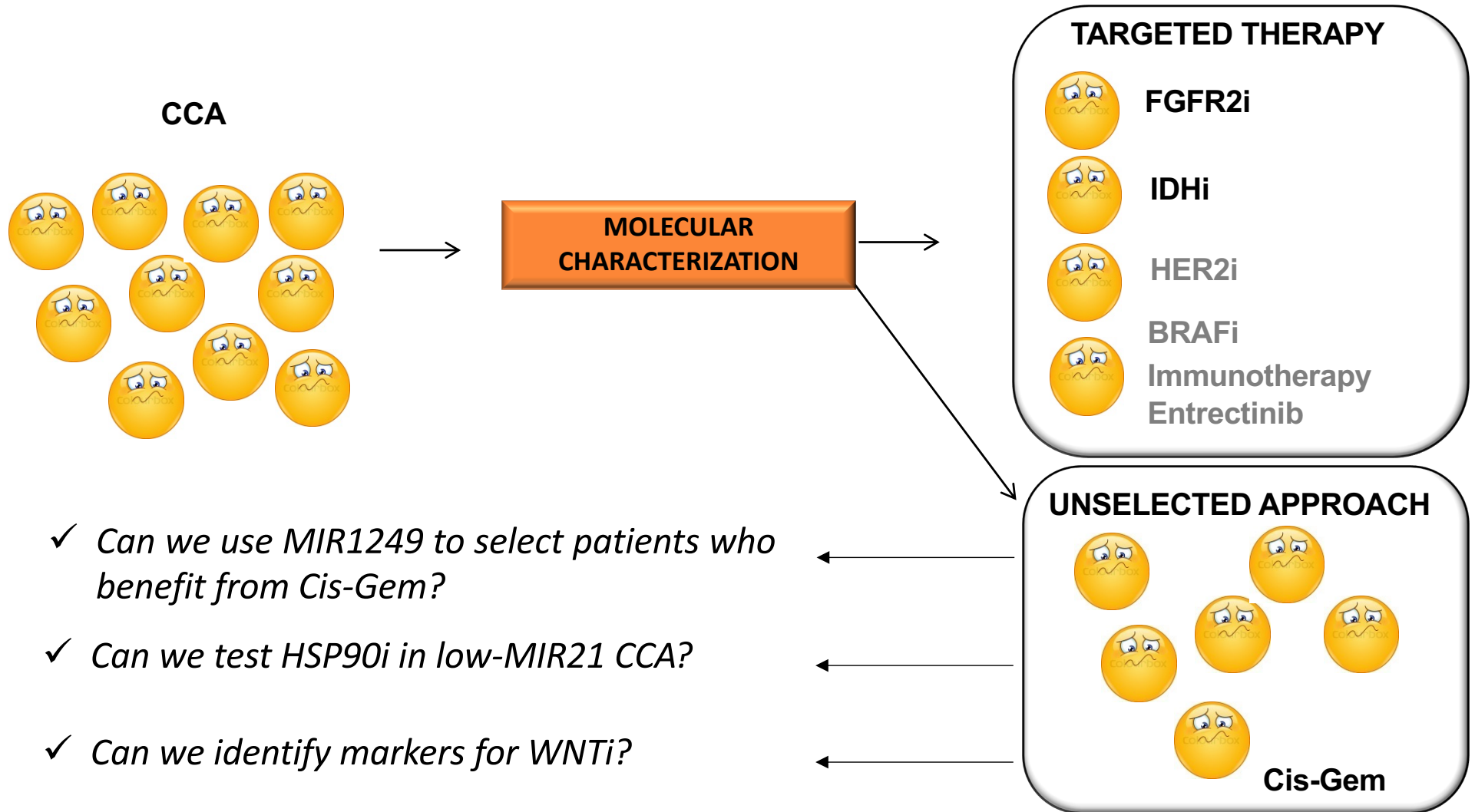
MIR21 expression was modulated in a PDO-xenograft with a doxycycline-inducible diet



Specificity of MIR21 to the HSP90 pathway was due to the targeting of DNAJB5



Expanding precision oncology beyond mutational status



Can ncRNAs be downstream of WNT pathway in liver cancer?

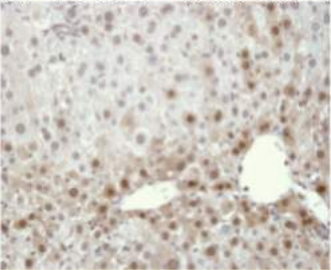
HCC
Apc fl/fl mice



NORMAL LIVER
Apc +/+ mice



Apc^{fl/fl}/Cre



b-catenin in the nuclei

Wnt pathway ↑

Buchert M, PLoS Genetics 10

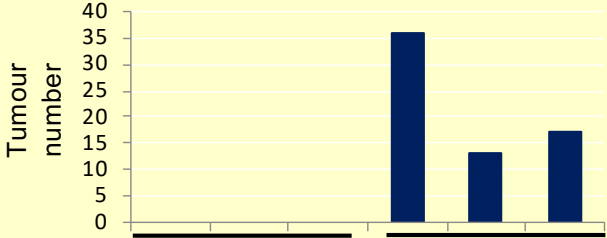
HCC
DEN treated mice



NORMAL LIVER
untreated mice



Tumour number



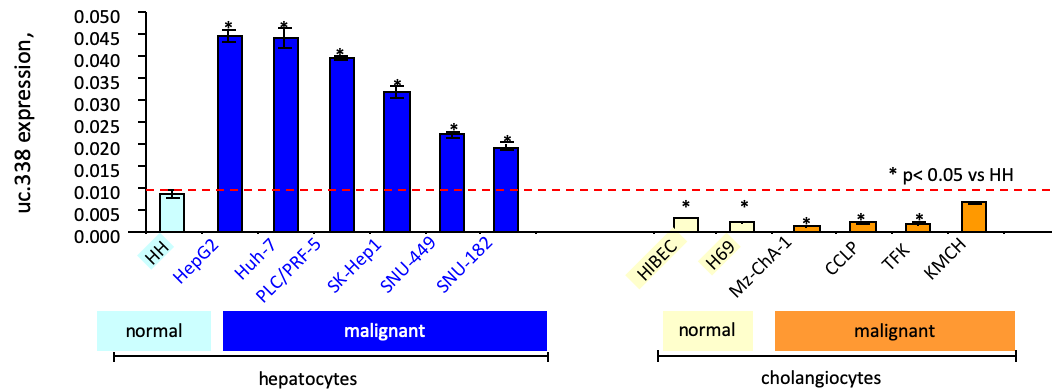
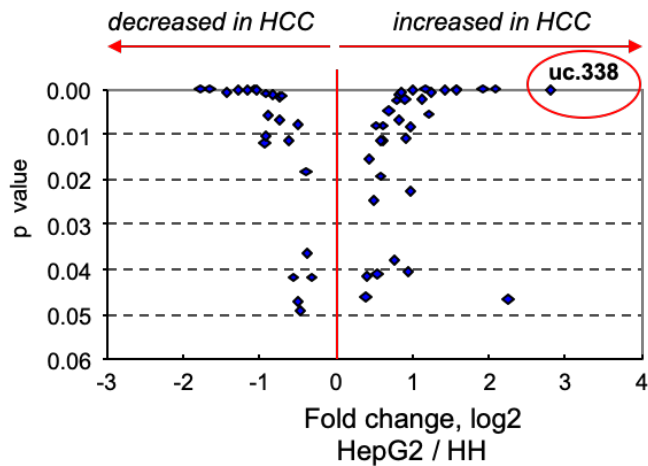
Group	Tumour number
untreated	0
40ug DEN as pups	35
40ug DEN as pups	13
40ug DEN as pups	17

untreated 40ug DEN as pups

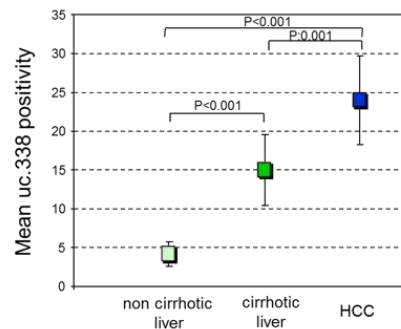
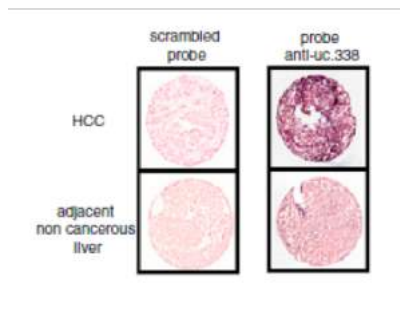
Global gene expression profiling
lncRNA
mRNA
miRNA

Transcribed-Ultraconserved Regions (T-UCR): long non-coding RNAs conserved across species

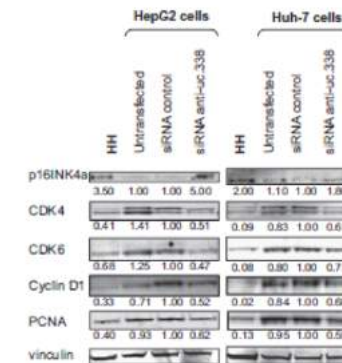
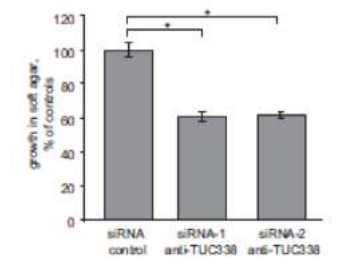
T-UCR are aberrantly deregulated in liver cancer cells



T-UCR deregulation increases with malignant transformation



T-UCR deregulation affects cell growth



Can T-UCRs be downstream of Wnt pathway?

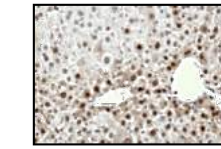
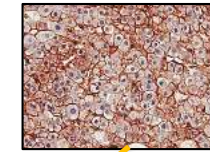


WNT-dependent liver tumours

NORMAL LIVER
Apc +/+ mice

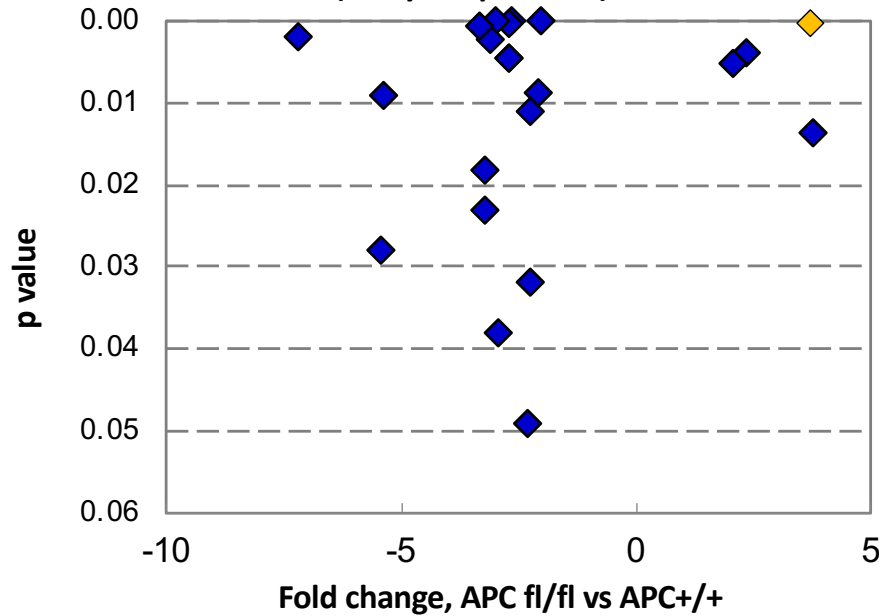
HCC
Apc fl/fl mice

DEN-induced HCC



Buchert, PLOS Genet 10

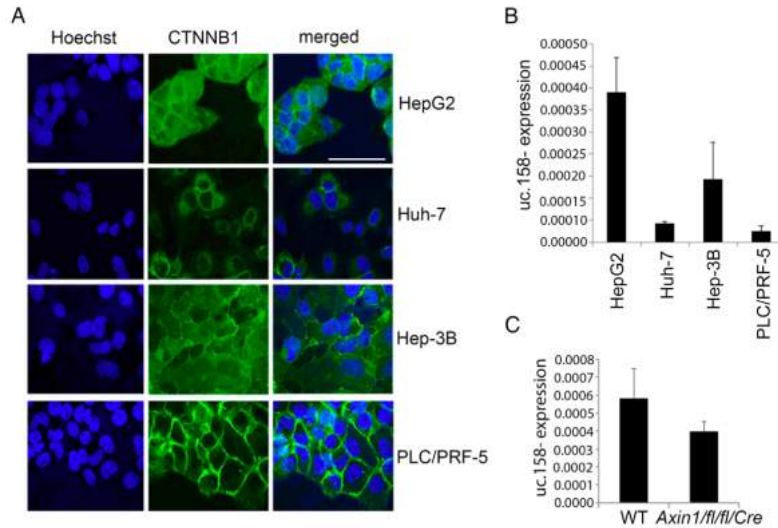
Profiling T-UCR expression
(Arraystar platform)



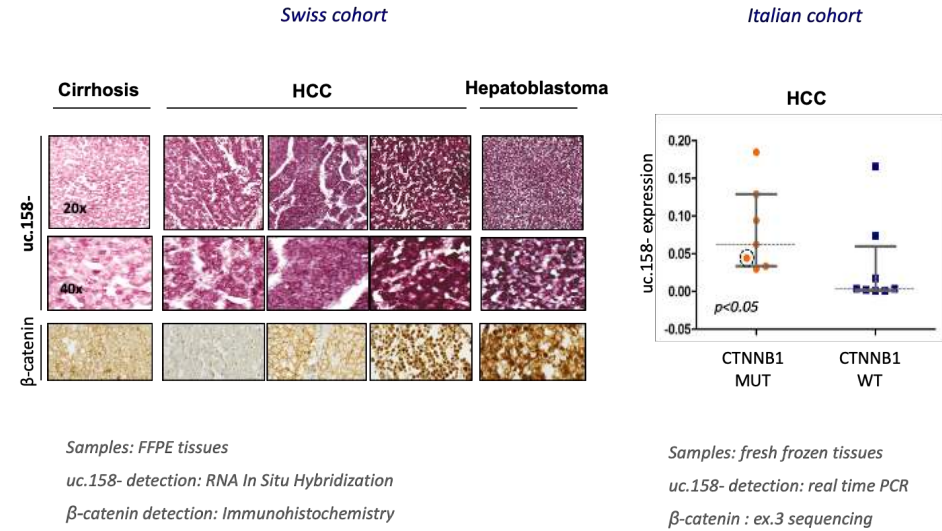
T-UCR	APC fl/fl vs APC +/+	APC fl/fl vs DEN	Genomic location
uc.158 -	3.73	2.21	Intergenic
uc.196+	-2.27	-6.4	Intergenic
uc.82 -	-2.68	-2.62	Intergenic
uc.455 +	-5.43	-3.65	overlap RBM39

uc.158- expression is specific for β -catenin dependent tumours and modulate cellular growth and invasion

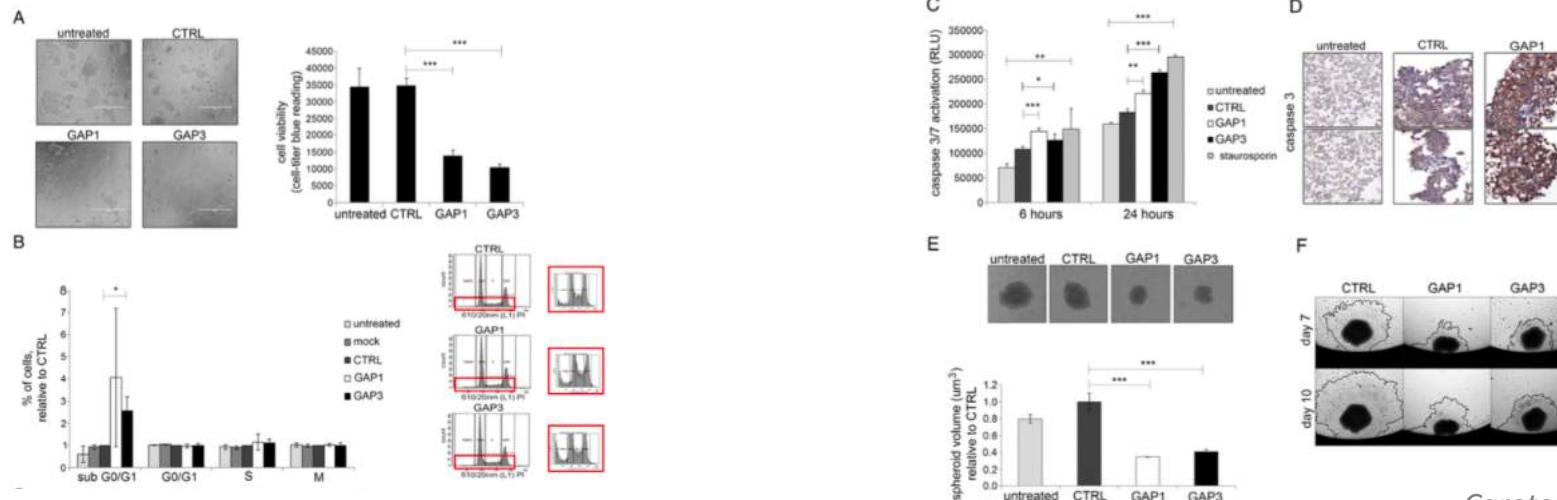
In vitro



In vivo



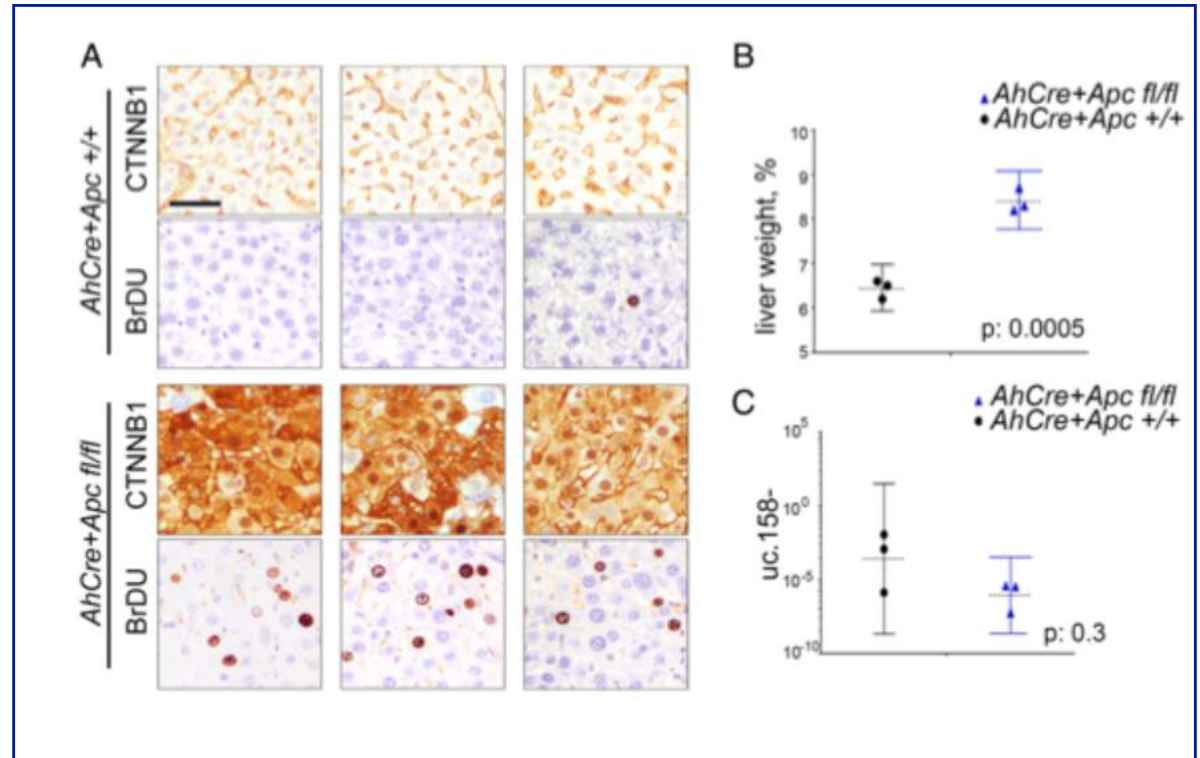
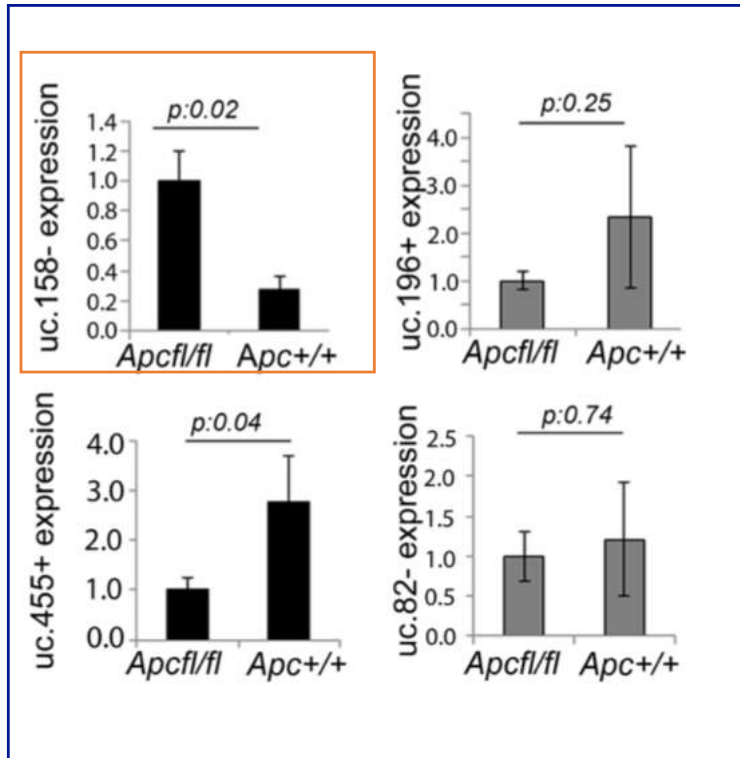
Biological Effects



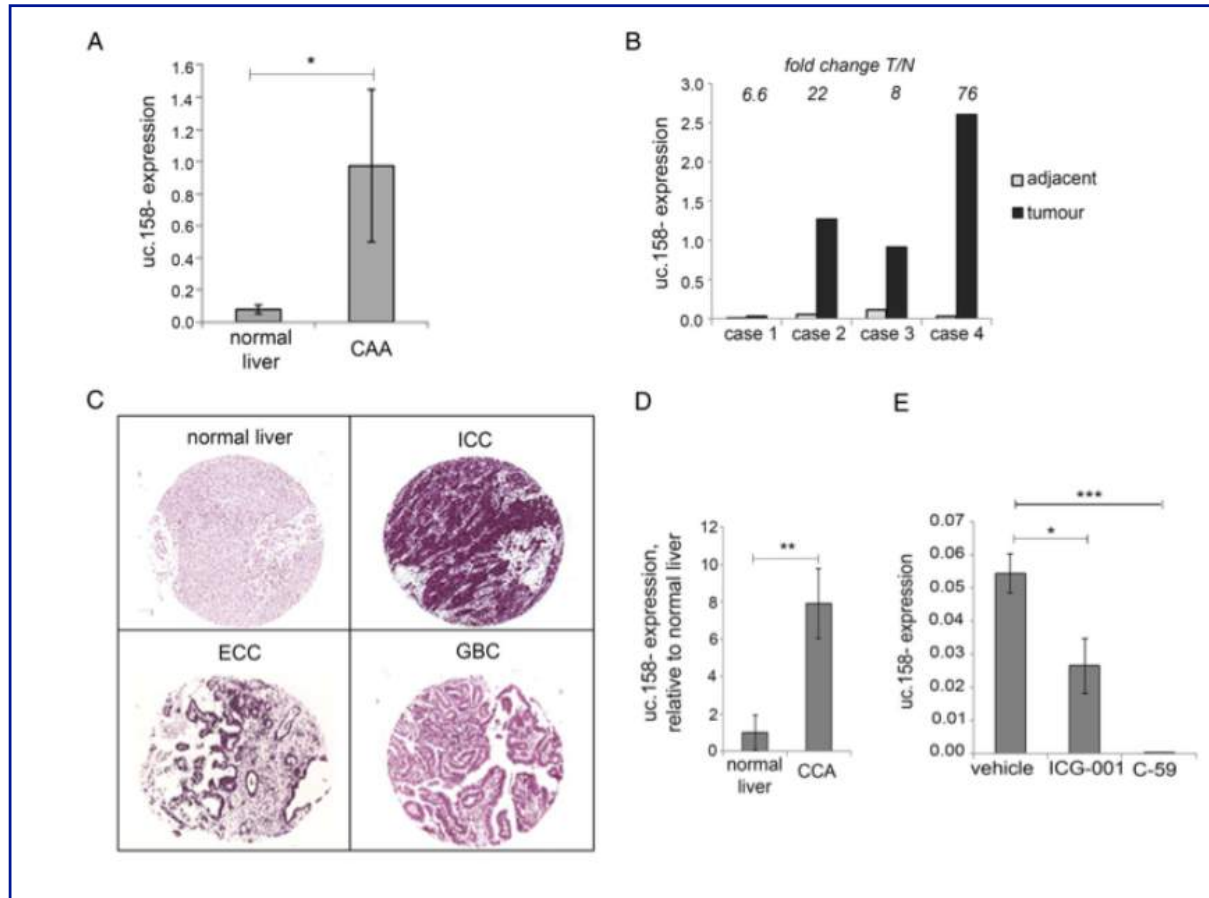
uc.158- was induced only in WNT-dependent malignant transformation

uc.158- was increased in WNT-dependent liver cancer

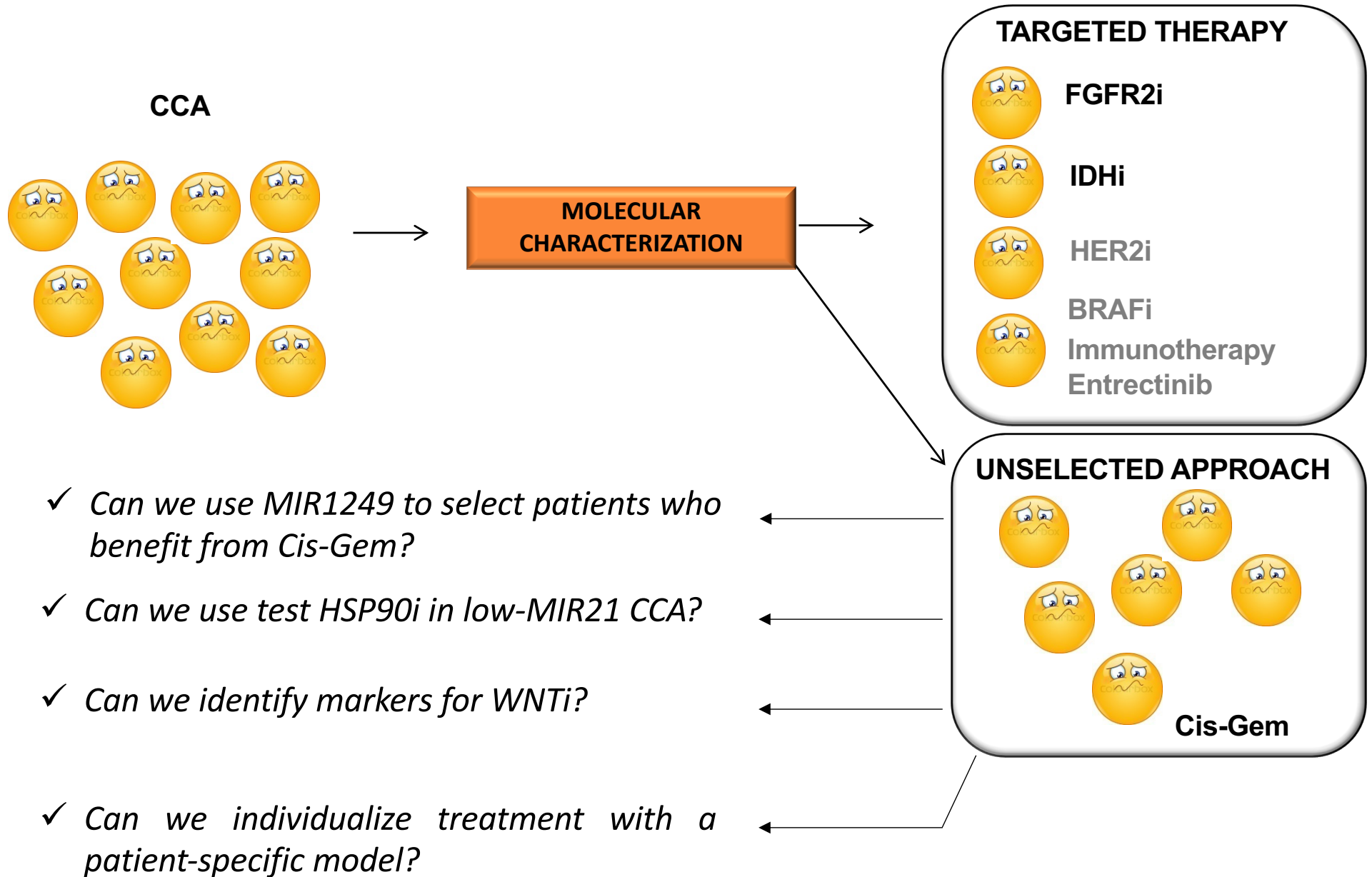
uc.158- does not change in WNT-dependent liver cell proliferation



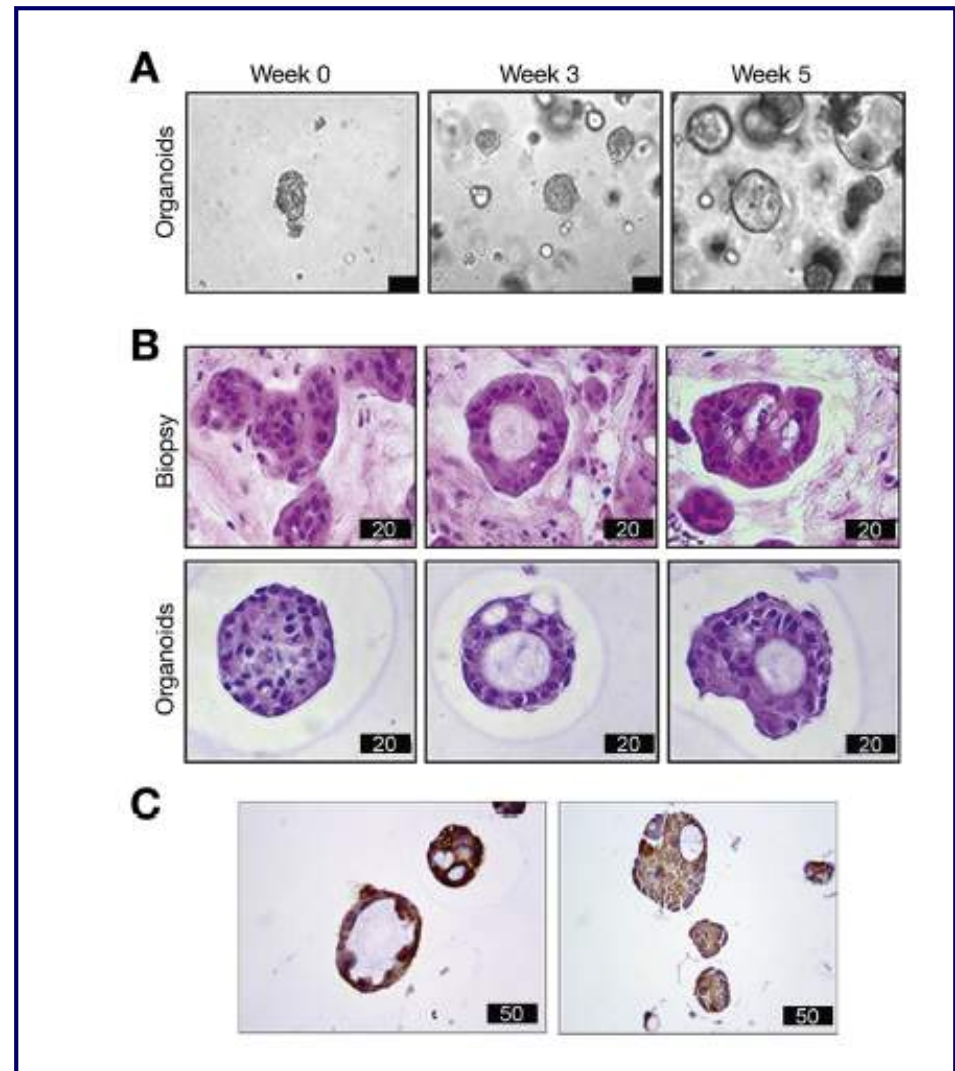
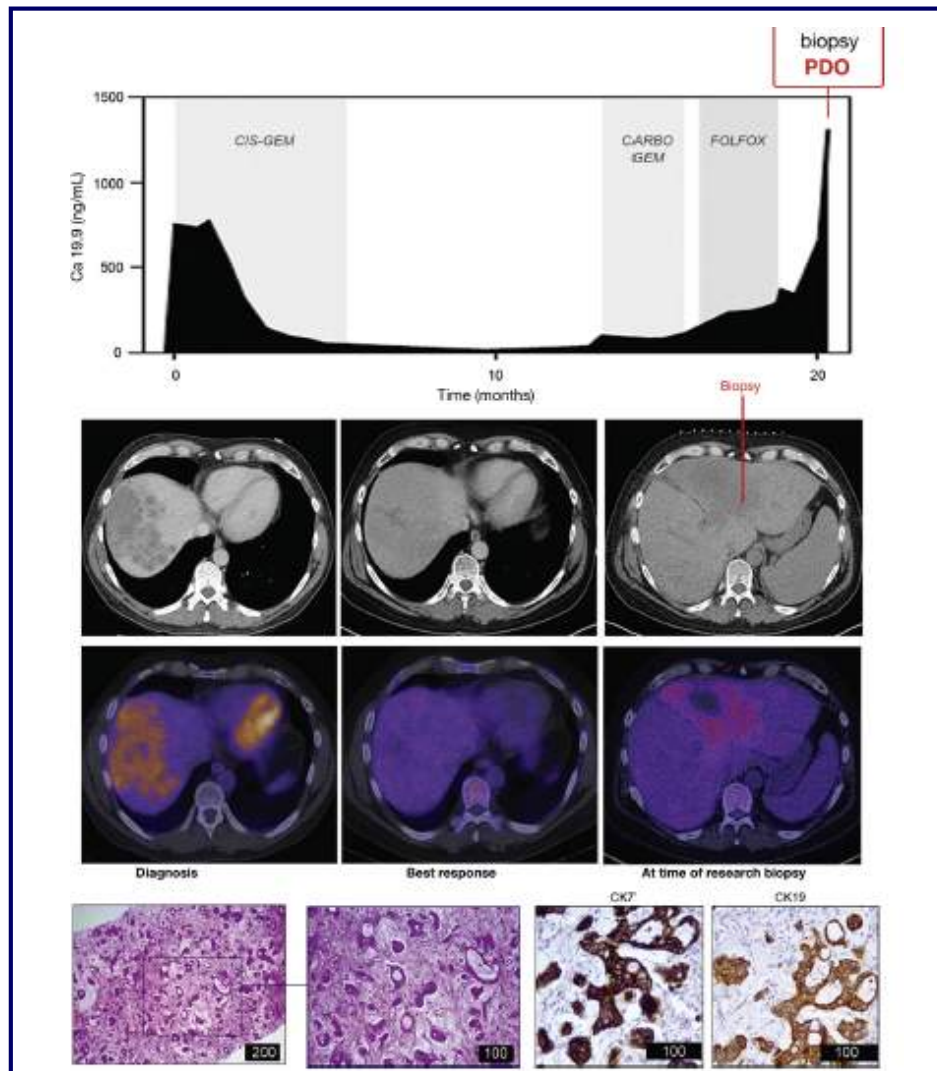
uc.158- is upregulated in iCCA



Expanding precision oncology beyond mutational status

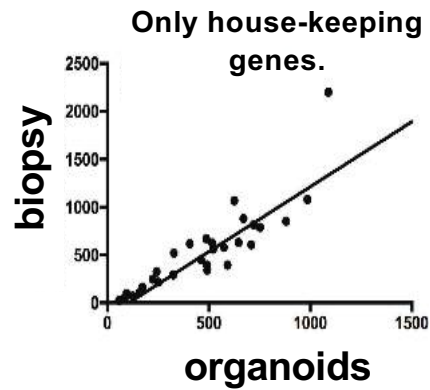


Advanced CCA PDOs recapitulate pathological phenotype of source tissue

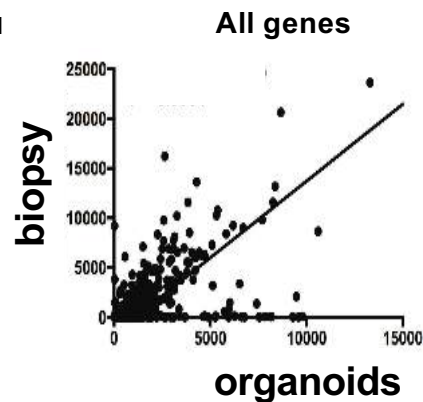


Advanced CCA PDOs recapitulate genomic landscape of source tissue

TRANSCRIPTOMIC (nanosttring analysis)

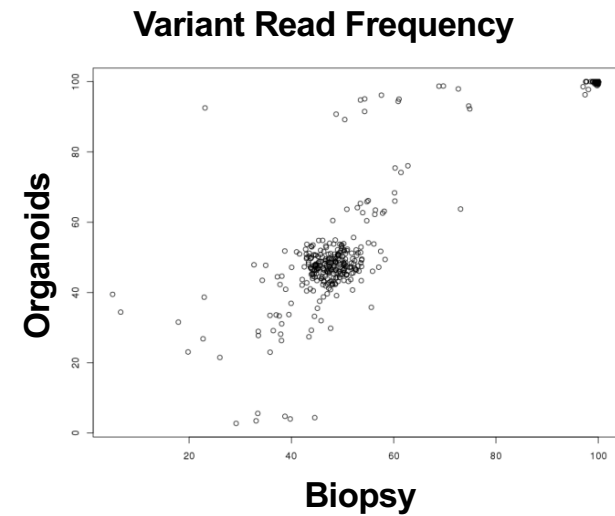


r: 0.91 [0.82-0.96]
p<0.0001



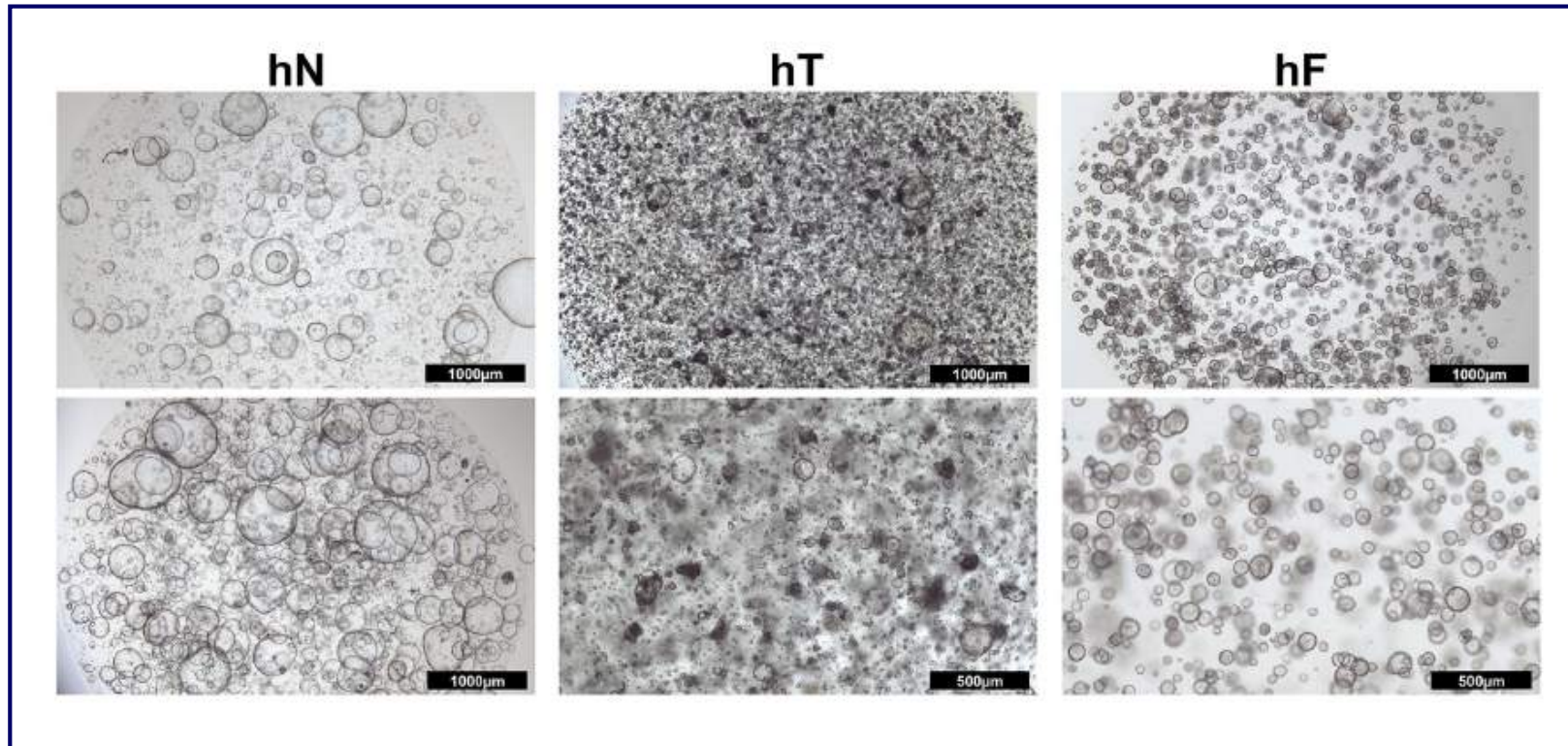
r: 0.61 [0.56-0.65]
p<0.0001

GENETIC (NGS)



r: 0.94
p < 0.00001)

PDO can be derived from pancreatic cancer (resection and EUS-FNB)

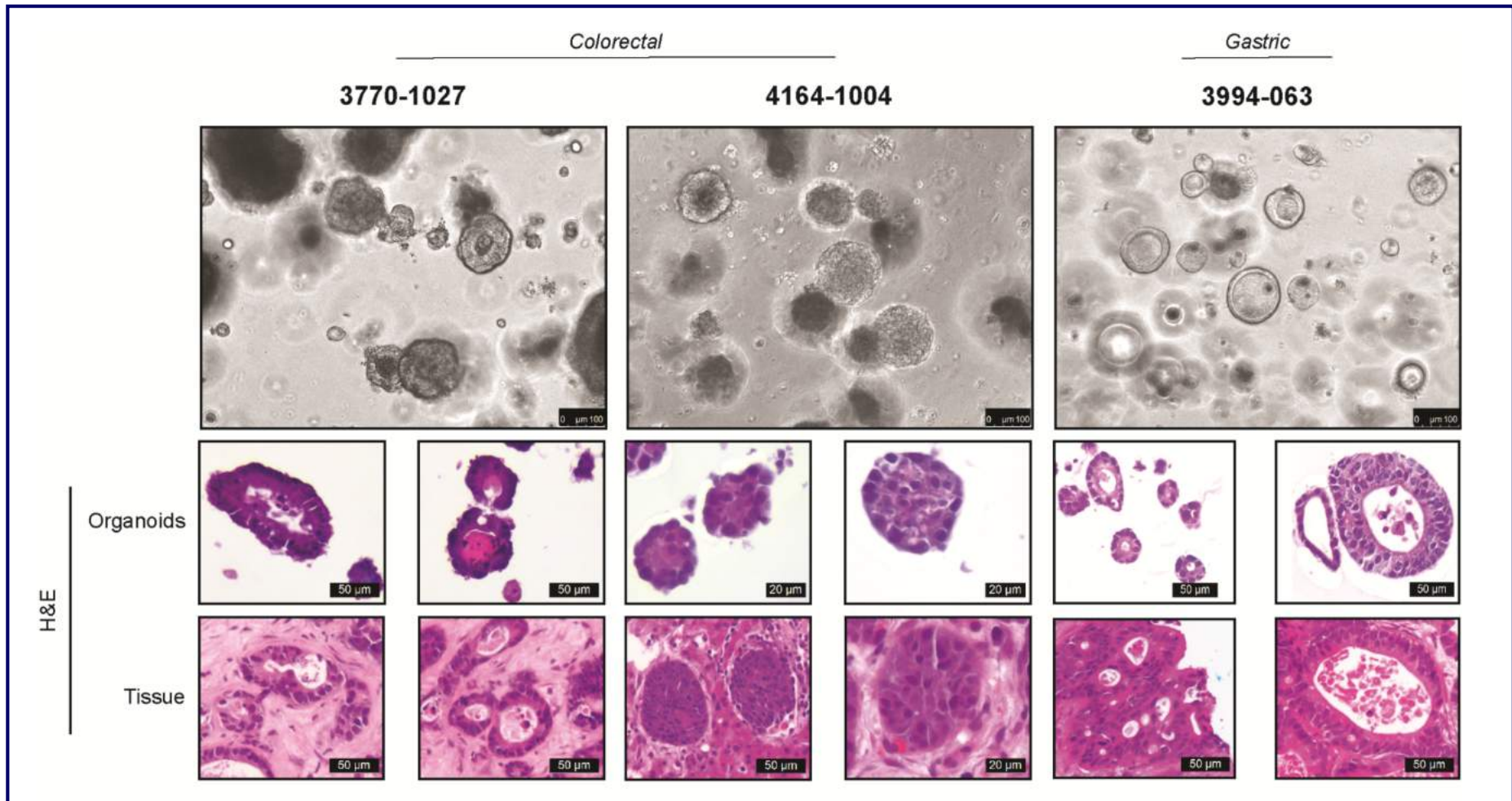


Surgical specimen:
FNB:

78%
72%

PDOs establishment can be escalated into the generation of a biobank

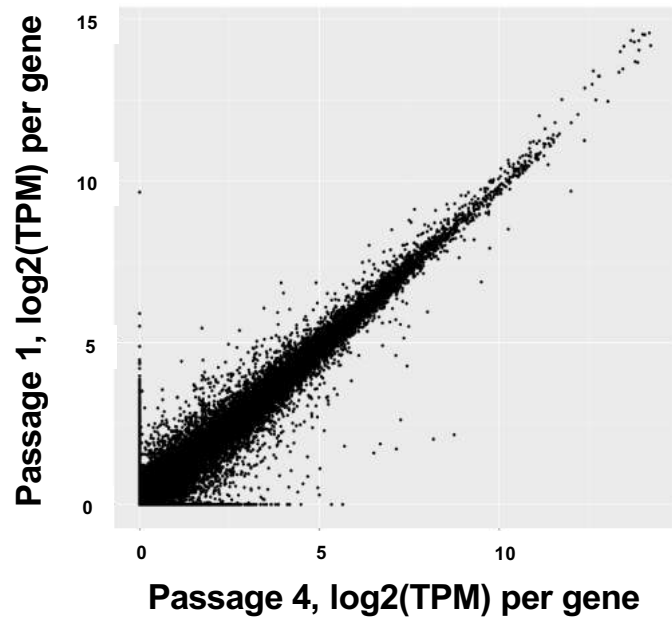
Efficiency rate of PDO establishment: 70% in the clinical setting



PDOs maintain the phenotype over time

RNA-seq

Advanced CCA PDO

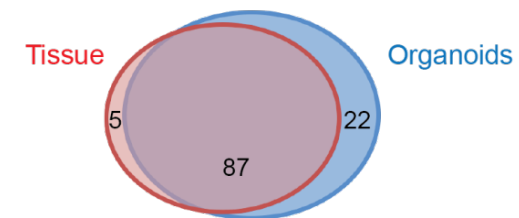
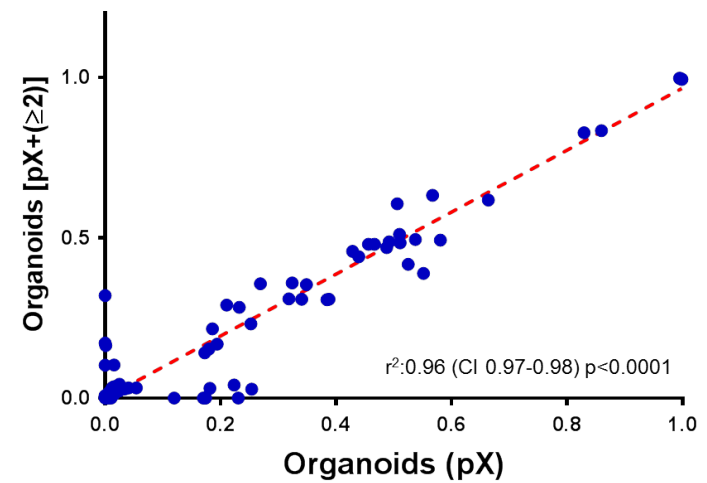


Pearson correlation is 0.9
p-value < 2.2e-16).

In collaboration with J. Andersen

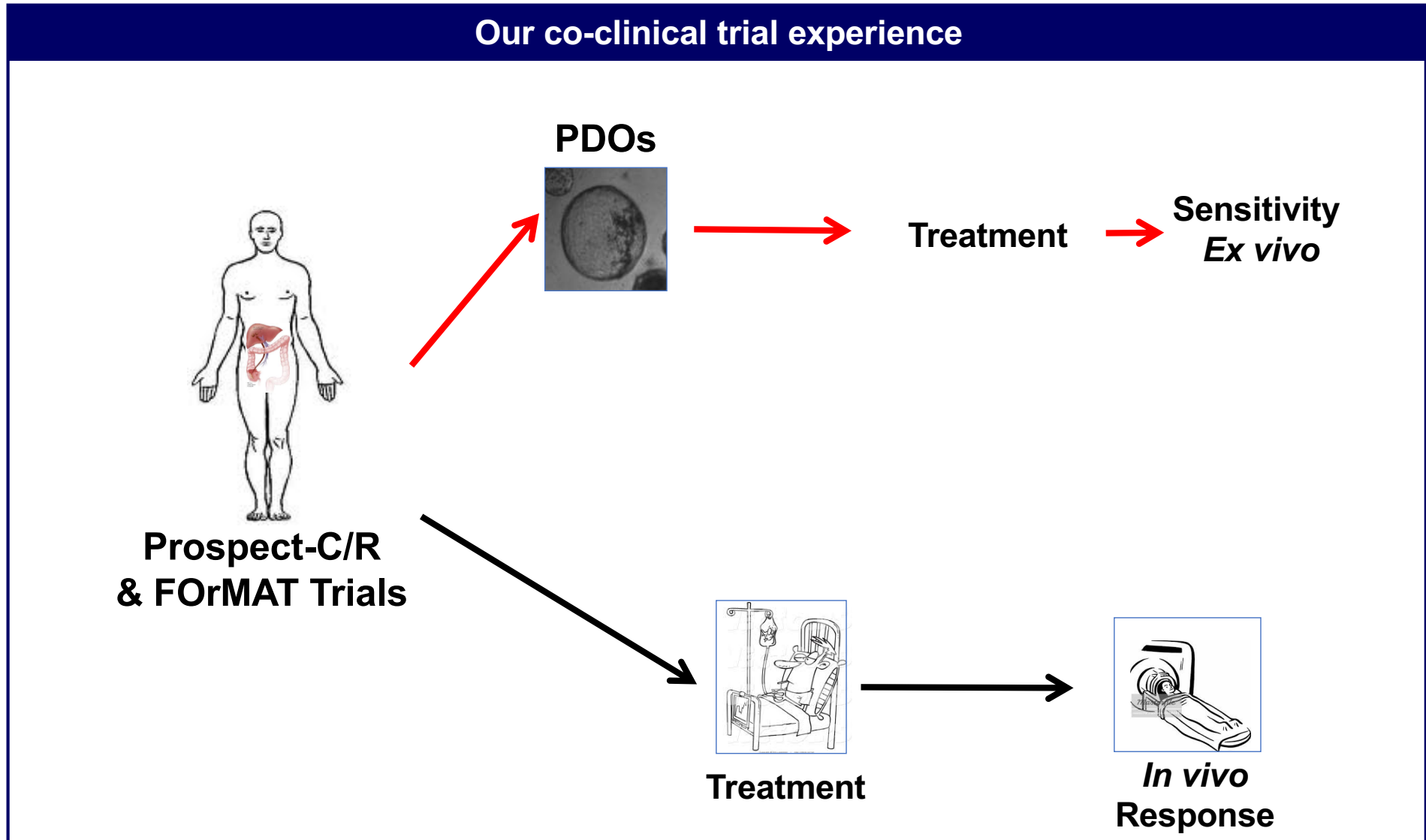
Mutational profile

Bio-bank of advanced GI cancers



Vlachogiannis, Science 2018

PDOs can be used for “live” drug screening

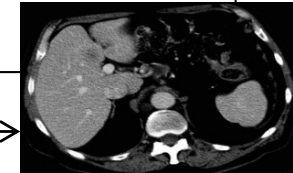
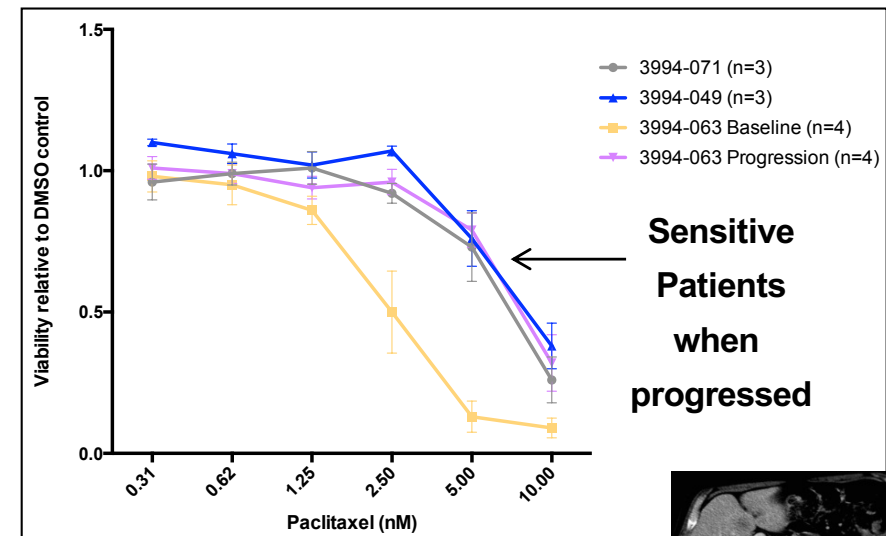
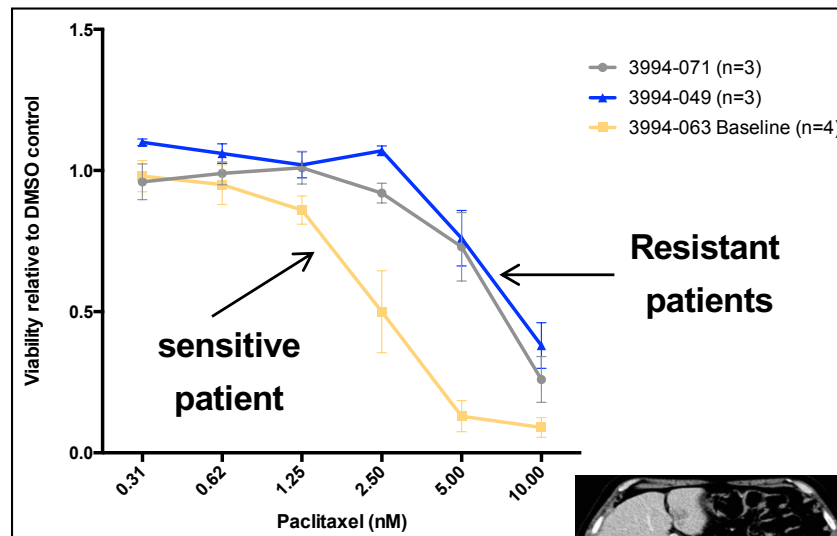


PDOs can be used for “live” drug screening

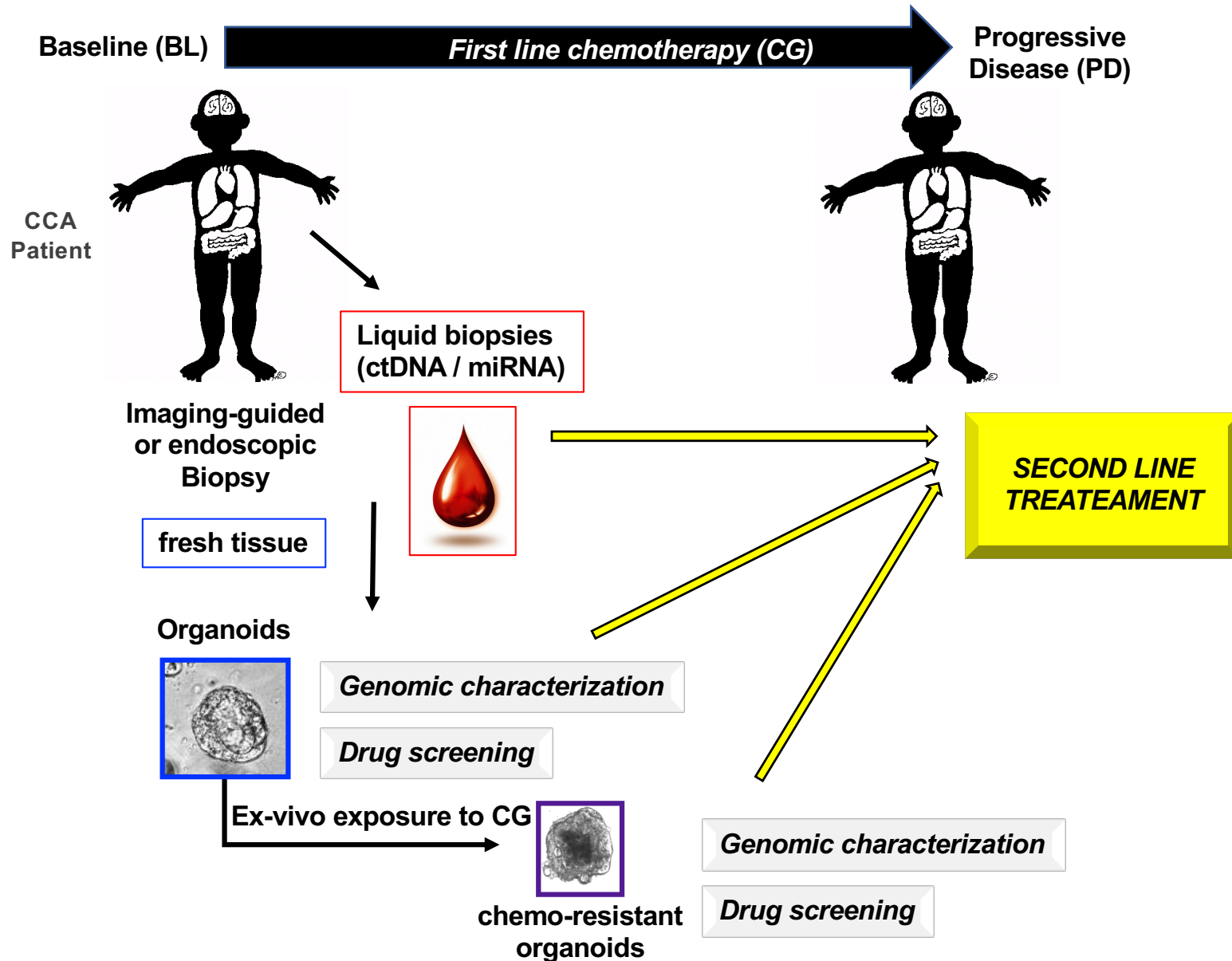
PDOs mimic response in the clinic

CHEMOTHERAPY

- Three metastatic gastric cancer FORMAT patients:
 - 3994-049 (Paclitaxel Resistant)
 - 3994-071 (Paclitaxel Resistant)
 - 3994-063 (Paclitaxel Sensitive)



A true pathway to have science at patients' service





Patients and families

University of Glasgow

Owen Sansom

Jeff Evans

Andrew Biankin



LKAS

stands for
Lord Kelvin Adam Smith



Abbreviations.com



NHS
National Institute for
Health Research



Acknowledgment

The Institute of Cancer Research- The Royal Marsden Pietro Carotenuoto

Maria C Previdi

Maya Raj

Max Salati

Michele Ghidini

Andrea Lampis

Somaieh Hedayat

George Vlachogiannis

Ian Huntingford

Jens C Hahne

Andrea Sottoriva

Anguraj Sadanandam

Vladimir Kirkin

Paul Workman

Nicola Valeri

Raj Chopra

David Cunningham

Ian Chau

Naureen Starling

David Watkins

Francesco Sclafani

Khurum Khan

Michalarea Vasiliki

Humanitas Cancer Centre

Llorenza Rimassa

Armando Santoro

Massimo Roncalli

Guido Torzilli

Cremona Hospital

Michele Ghidini

University of Edinburgh

Stuart Forbes

Luke Boulter

Rachel Guest

University of Bellinzona

Luciano Cascione

Mayo Clinic

Tushar Patel

BIRC Copenhagen

Jesper Andersen

Chirag Nepal

UCL

Steve Pereira

John Bridgewater

University of Birmingham

Yuk Ting Ma

University of Verona

Aldo Scarpa

Michele Simbolo

University of Padova

Matteo Fassan

Massimo Rugge

Umberto Cillo

University of Liverpool

Daniel Palmer

University of Cardiff

Trevor Dale

Roma Sapienza

Domenico Alvaro

Vincenzo Cardinale

University of Chieti

Angelo Veronese

Asahikawa University

Kenji Takahashi

National Institute of Infectious Disease Tokyo

Tetsuro Suzuki